

# Phase and Amplitude Dynamics in Large Systems of Coupled Oscillators: Growth Heterogeneity, Nonlinear Frequency Shifts and Cluster States

Wai Shing Lee, Edward Ott and Thomas M. Antonsen Jr.

*Institute for Research in Electronics and Applied Physics,  
University of Maryland, College Park, Maryland 20742, USA*

## Abstract

This paper addresses the behavior of large systems of heterogeneous, globally coupled oscillators each of which is described by the generic Landau-Stuart equation, which incorporates both phase and amplitude dynamics of individual oscillators. One goal of our paper is to investigate the effect of a spread in the amplitude growth parameter of the oscillators and of the effect of a homogeneous nonlinear frequency shift. Both of these effects are of potential relevance to recently reported experiments. Our second goal is to gain further understanding of the macroscopic system dynamics at large coupling strength, and its dependence on the nonlinear frequency shift parameter. It is proven that at large coupling strength, if the nonlinear frequency shift parameter is below a certain value, then there is a unique attractor for which the oscillators all clump at a single amplitude and uniformly rotating phase (we call this a single-cluster “locked state”). Using a combination of analytical and numerical methods, we show that at higher values of the nonlinear frequency shift parameter, the single-cluster locked state attractor continues to exist, but other types of coexisting attractors emerge. These include two-cluster locked states, periodic orbits, chaotic orbits, and quasiperiodic orbits.

PACS numbers:

Systems of coupled oscillators occur in a very wide variety of applications. Often interaction between the dynamical evolution of the oscillator phases and amplitudes is an important issue. The simplest model of such dynamics is that of a globally coupled system of Landau-Stuart equations [1]. While this system is very basic, due to the large space of possibilities for its parameters and their probability distribution functions, a complete understanding of the system is lacking. Here, motivated by recent experiments [2], we consider parameter dependences not previously investigated. We also investigate the reason for the common occurrence of “locked states” (constant amplitude and sinusoidal oscillation) observed in previous studies when the coupling is large, why non-locked-state attractors occur at sufficiently large values of the nonlinear frequency shift parameter, and what types of attractors can occur at large coupling and large nonlinear frequency shift.

## I. INTRODUCTION

The interaction of many coupled dynamical units is a common theme across a broad range of scientific disciplines. Within this general theme, the issue of determining conditions for the emergence of macroscopic cooperative behavior and of determining the nature of this behavior is of central importance [1, 3]. Examples include coupled lasers [4]-[6], Josephson junction circuits [7, 8], interacting yeast cells [9, 10], pacemaker cells in the heart [11], pedestrian induced oscillation of footbridges [12]-[14], chemically reacting systems [2, 15], circadian rhythms [16], and many others.

A very useful simplified framework for beginning to understanding phenomena observed in these situations is the phase oscillator description. In the phase oscillator description the dynamical units are assumed to be oscillatory with fixed amplitude. Thus, the state of each individual unit can be specified solely by a phase angle  $\theta$ , and the evolution of oscillator  $i$  is taken to be determined by its present state  $\theta_i$  and by the states  $\theta_j$  of the other oscillators ( $j \neq i$ ). The simplest model of this type was originally put forward by Kuramoto in 1975 and has proven to be an extremely useful paradigm for understanding this general type of system [17]-[21]. In addition, the Kuramoto model has also served as a basis for formulating related phase oscillator models appropriate to a wide variety of

situations (e.g., see Ref. [22]). The basic question addressed by the Kuramoto model is the competition between the synchronizing effect of coupling and the desynchronizing effect of different natural frequencies of the individual oscillators. The principal result [17]-[22] coming from the solution of the Kuramoto model is that, in the limit of a large number of oscillators, this competition is resolved by a transition, whereby there is a critical coupling strength below which the oscillations of individual oscillators occur with random phase and there is no macroscopic population-wide oscillation, while above which oscillators begin to develop phase coherence, and globally-averaged population-wide oscillation emerges.

A drawback of the phase oscillator description is that, by its definition, it excludes the effect of amplitude dynamics and the possible coupling of amplitude dynamics with phase dynamics. Another useful oscillator model incorporating both amplitude and phase dynamics is based on the normal form of an isolated system near a Hopf bifurcation,

$$\frac{dz}{dt} = (\alpha + i\omega)z - (\beta + i\gamma)|z|^2z, \quad (1)$$

also referred to as a Landau-Stuart oscillator [1]. In (1)  $z$  is complex with  $|z|$  and the angle of  $z$  representing the amplitude and phase of the oscillator. The real parameter  $\alpha$  is the linear amplitude growth rate of the oscillations, with  $\alpha > 0$  for growth (and  $\alpha < 0$  for damping). The Hopf bifurcation occurs as  $\alpha$  passes through zero. The other real parameters  $\omega, \beta, \gamma$  respectively characterize the small-amplitude natural frequency of the oscillator, and the finite amplitude nonlinear shifts of the small amplitude growth rate and frequency. The bifurcation is supercritical if  $\beta > 0$  (the nonlinear term saturates growth) and subcritical (hysteretic) if  $\beta < 0$  (the nonlinear term enhances growth). Here we will only deal with the supercritical case [in the subcritical case, if  $\alpha > 0$ , orbits typically go far from  $z = 0$ , thus invalidating the expansion resulting in (1)]. For  $\alpha < 0$ , Eq. (1) has as its stable solution  $z = 0$ . For  $\alpha > 0$ ,  $z = 0$  is unstable, and (1) results in an attracting limit cycle attractor,

$$z = \sqrt{\frac{\alpha}{\beta}} \exp \left[ i \left( \omega - \frac{\gamma\alpha}{\beta} \right) t + \theta_0 \right], \quad (2)$$

which traces a circular orbit about the origin of the complex  $z$ -plane. In general, the normal form oscillator parameters  $(\alpha, \omega, \beta, \gamma)$  derived from the physical system under study will depend on some set,  $\mathbf{p} = (p^{(1)}, p^{(2)}, \dots, p^{(n)})^T$ , of physical parameters for that system. That is,  $[\omega, \alpha, \beta, \gamma] = [\omega(\mathbf{p}), \alpha(\mathbf{p}), \beta(\mathbf{p}), \gamma(\mathbf{p})]$ .

We are interested in the situation, also studied in Refs. [23]-[29], where many oscillators of the form of Eq. (1) are coupled together and where each such oscillator (indexed by a subscript  $i = 1, 2, \dots, N \gg 1$ ) may have a different parameter set. That is, if oscillator  $i$  has parameter set  $\mathbf{p}_i$ , then

$$[\omega_i, \alpha_i, \beta_i, \gamma_i] = [\omega(\mathbf{p}_i), \alpha(\mathbf{p}_i), \beta(\mathbf{p}_i), \gamma(\mathbf{p}_i)]. \quad (3)$$

If the value of  $\mathbf{p}$  is regarded as assigned randomly from oscillator to oscillator according to some probability distribution function (pdf), then that will induce a corresponding pdf  $\hat{G}$  of the parameters  $[\omega, \alpha, \beta, \gamma]$ , such that

$$\hat{G}(\omega, \alpha, \beta, \gamma) d\omega d\alpha d\beta d\gamma \quad (4)$$

represents the fraction of oscillators with parameters  $\omega, \alpha, \beta, \gamma$  in the range  $\omega \in [\omega, \omega + d\omega]$ ,  $\alpha \in [\alpha, \alpha + d\alpha]$ ,  $\beta \in [\beta, \beta + d\beta]$ ,  $\gamma \in [\gamma, \gamma + d\gamma]$ , and applicable in the limit  $N \rightarrow \infty$ , where  $N$  is the number of oscillators.

Considering this general problem, one would like to know how the system behavior depends on the distribution function  $\hat{G}(\omega, \alpha, \beta, \gamma)$ . However, as  $\hat{G}$  is a distribution in the four variables  $\omega, \alpha, \beta, \gamma$ , this is clearly too big a problem to address in full generality. Here we will pursue a more modest program. In particular, the questions we address are partly motivated by the experimental work in Ref. [2]: (i) what is the effect of spread in  $\alpha$  allowing the simultaneous presence of dead ( $\alpha < 0$ ) and active ( $\alpha > 0$ ) oscillators in the uncoupled state, and (ii) what is the effect of a nonlinear frequency shift  $\gamma$  (for simplicity, we treat the oscillators as all having the same  $\gamma$ ), and (iii) how we can understand certain types of simple nonlinear behavior often observed in these systems when the coupling strength between oscillators is large?

## II. FORMULATION, BACKGROUND AND OUTLINE

We assume  $\beta$  and  $\gamma$  are the same for all oscillators,  $\beta_i = \bar{\beta}$  and  $\gamma_i = \bar{\gamma}$ . Furthermore, we scale  $\bar{\beta}$  to one by a proper normalization of  $z_i$  ( $z_i \rightarrow z_i/\sqrt{\bar{\beta}}$ ). Thus

$$\hat{G}(\omega, \alpha, \beta, \gamma) = G(\omega, \alpha) \delta(\beta - 1) \delta(\gamma - \bar{\gamma}). \quad (5)$$



If  $\omega$  and  $\alpha$  are uncorrelated in their variation from oscillator to oscillator, then  $G$  is of the form

$$G(\omega, \alpha) = g(\omega)h(\alpha). \quad (6)$$

In what follows we assume that Eq. (6) holds [30], and that  $g(\omega)$  is symmetric and monotonically decreasing with respect to its maximum value, which we can take to be located at  $\omega = 0$  (if the maximum of  $g(\omega)$  occurred at some non-zero value,  $\omega = \bar{\omega}$ , then the location of the maximum can be shifted to zero by the change of variables  $z = z'e^{i\bar{\omega}t}$ ,  $\omega' = \omega - \bar{\omega}$ ).

For (1) with  $\beta_i = 1$ ,  $\gamma_i = \bar{\gamma}$  and (6) specifying our ensemble of uncoupled oscillators, we now proceed to globally couple these ensemble members through a mean field,  $\langle z \rangle$ ,

$$\frac{dz_i}{dt} = (\alpha_i + i\omega_i)z_i - (1 + i\bar{\gamma})|z_i|^2z_i + \Gamma\langle z \rangle, \quad (7a)$$

$$\langle z \rangle = \frac{1}{N} \sum_{j=1}^N z_j, \quad (7b)$$

where the parameter  $\Gamma$  measures the strength of the coupling and is assumed real and positive,  $\Gamma \geq 0$  (some previous studies have considered complex coupling constants, e.g., Refs. [37]-[40]). We will sometimes refer to  $\langle z \rangle$  as the “order parameter” because whether or not there is global collective behavior for  $N \rightarrow \infty$  corresponds to whether  $|\langle z \rangle| > 0$  or  $\langle z \rangle = 0$ . See Refs. [23]-[29] for previous related work on large coupled systems of Landau-Stuart equations. In many of these previous works [23]-[27], the coupling term is written as  $K(\langle z \rangle - z_i)$  in place of  $\Gamma\langle z \rangle$ . This choice is simply related to ours by the transformation  $\alpha_i = \hat{\alpha}_i - K$ ,  $\Gamma = K$ . We prefer the parametrization in Eq. (7) because one of our principal motivations will be experiments [2] where it can be plausibly argued that quantities analogous to  $\Gamma$  and the average value of  $\alpha_i$  (denoted  $\bar{\alpha}$ ) can be varied essentially independently. More generally, in real large coupled oscillator systems familiar to us, coupling between the oscillators typically results from physical processes distinct from those determining the properties of the individual oscillators (as in Ref. [2]), and the parametrization in Eq. (7) is therefore the appropriate one. Use of the form (7) (rather than (8) below) will be important for our considerations of the large coupling limit in Sec. IX. In addition, in Refs. [23]-[27] it was considered that  $\hat{\alpha}_i$  was the same positive constant for all  $i$ ,  $\hat{\alpha}_i = \hat{\alpha}$ , and furthermore that

$\bar{\gamma} = 0$ . Parameter and time normalizations were then chosen to transform  $\hat{\alpha}$  to 1, yielding, in place of (7)

$$\frac{dz_i}{dt} = (i\omega_i + 1 - |z_i|^2)z_i + K(\langle z \rangle - z_i), \quad (8)$$

where the coupling parametrization form  $K(\langle z \rangle - z_i)$  was used. We, however, will be interested in the effect of a spread in  $\alpha_i$  with the possibility of the simultaneous occurrence of positive and negative  $\alpha_i$  for different  $i$ , and also in the effects of nonlinear frequency shift  $\bar{\gamma} \neq 0$ .

One motivation for this study is the recent paper, Ref. [2], which describes experiments in which many ( $\sim 10^4/cm^3$ ) specially designed small porous particles are continuously and rapidly mixed in a catalyst-free Belousov-Zhabotinsky reaction mixture. The catalyst for the reaction is immobilized on the small porous particles, each of which can potentially serve as an effective chemical oscillator. Oscillations in the chemical states of the particles are visualized as the color of the particles oscillates between red and blue. The particle density serves as a parameter analogous to our coupling constant  $\Gamma$ , while regulation of the stirring rate effectively provides a control analogous to control of the mean oscillator growth rate,

$$\bar{\alpha} = \int \alpha h(\alpha) d\alpha. \quad (9)$$

Because the process by which the particles are prepared is not perfect, it is expected that there will be substantial spread in their parameters, and in particular in  $\omega$  and  $\alpha$ . These spreads are of particular interest because: (i) spread of oscillator frequencies is the essential feature leading to the transition from incoherently oscillating units to macroscopic oscillation in the Kuramoto model, and (ii) the parameter  $\alpha$  determines whether individual particles, when uncoupled, oscillate ( $\alpha > 0$ ) or do not oscillate ( $\alpha < 0$ ). In the case  $\alpha < 0$  the attractor for Eq. (1) is the fixed point  $z = 0$ , often referred to as “oscillator death”. With reference to point (ii), because of the spread in  $\alpha$ , in some range of stirring rates, we can expect a situation like that shown schematically in Fig. 1, which depicts an uncoupled oscillator growth rate pdf  $h(\alpha)$  yielding substantial fractions of the particles in the oscillating and dead states. As  $\bar{\alpha}$  increases from very negative values,  $(-\bar{\alpha}) \gg \delta\alpha$  (analogous to low stirring rates in the experiment), to very positive values,  $\bar{\alpha} \gg \delta\alpha$  (analogous to high stirring rates), there is a continuous transition from predominantly dead to predominantly oscillatory dynamics of

the uncoupled oscillators. Another notable feature of these experiments is that the collective coherent frequency of oscillation exhibits a marked dependence on the oscillation amplitude through its dependence on the density of the porous particles at fixed stirring rate (e.g., the third panels in Fig. 2(a) and 2(b) of Ref. [2]). This is a strong indication that the nonlinear frequency shift  $\bar{\gamma}$  plays a significant role. It is notable that Ref. [2] developed a set of chemical rate equations that, when solved numerically, yield good agreement with the experiments. While this is a singular achievement, we are interested in obtaining additional understanding of the processes involved and in determining if it is generic. To the extent that qualitative behavior of our Landau-Stuart model mimics behavior observed in the particular experiment in Ref. [2], the typicality of the observed phenomena is strongly implied. Furthermore, if the above agreement holds, then any analytical results obtained for the Landau-Stuart model may lead to further understanding of these experimental phenomena. Thus it is our desire to employ the generic coupled Landau-Stuart model, Eqs. (7), to explore and understand the nature of the interplay between frequency spread, growth rate spread and nonlinear frequency shift. In this connection, it is worth noting that our work may be applicable to other experiments. Indeed, as described in Ref. [2], the chemical experiment was, at least partly, intended to mimic observed oscillator quorum-sensing in yeast populations [9, 10]. In addition, the basic stability analysis technique used here (Sect. III) is similar to that originally introduced in Refs. [26] and [27] can also be applied to other amplitude / phase oscillator systems, such as the laser system considered in Ref. [6].

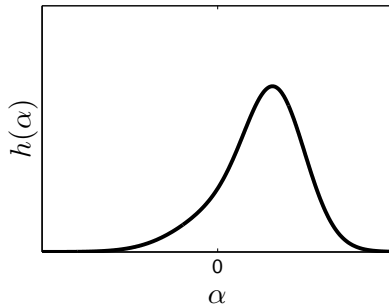


FIG. 1: Schematics of  $h(\alpha)$ .

We now give a brief review of the most important papers [23]-[29] related to our work. References [23]-[27] considered Eq. (8) (all oscillators have identical  $\alpha_i$  and  $\gamma_i = 0$ ) and examined the behavior as a function of the coupling constant  $K$  and the spread  $\sigma$  in the

oscillator frequencies. Shiino and Frankowicz [23] by a combination of numerical experiments and analysis obtain an approximate  $K - \sigma$  plane phase diagram. References [24, 25] examine the transition between “amplitude death” [31, 32] (i.e.,  $z_i = 0$  for all oscillators) and collective oscillation, explicitly obtaining analytical results for the boundary in  $K - \sigma$  space separating death and collective oscillation.

Matthews et al. [26, 27], in addition to presenting an extensive numerical exploration, also develop an analytical technique for handling the transition to globally coherent oscillation from phase-incoherent individual oscillation with  $|z_i| > 0$  (as in the Kuramoto transition [18]-[22]); thus this work was the first to include analysis of the effect of amplitude dynamics on this type of transition. In addition, another important result of Refs. [26, 27] was the numerical discovery that near the boundary in parameter space where the transition to collective behavior occurs, this collective behavior can be rather complex, including period doubling cascades, chaos, quasiperiodicity and hysteresis. Further, sufficiently far above the boundary it was found that steady oscillatory behavior prevails (as in the Kuramoto model).

Reference [28] introduces a situation that the authors call “aging” in which there are two populations, each described by an equation of the form of (7) (with  $\alpha_i = \hat{\alpha} - K$  and  $\Gamma = K$ ); the “old” population has  $\hat{\alpha}_i = -\hat{\alpha}_o < 0$  (corresponding to amplitude death at  $K = 0$ ), and the “young” population has  $\hat{\alpha}_i = \hat{\alpha}_y > 0$ ;  $\omega_i$  was taken to be the same constant  $\Omega$  for all old and young oscillators (see also [29] which allows distinct old and young natural frequencies,  $\omega_i = \Omega_o$  and  $\Omega_y$ ); and behavior was investigated as a function of the ratio of the populations of old relative to young. In the set up of Refs. [28, 29], due to the homogeneity of frequencies, the transition problem reduces to the analysis of two coupled Landau-Stuart equations.

Nonlinear behavior of large systems of *identical* Landau-Stuart oscillators was considered by Refs. [37]-[41], which highlight the possible occurrence of “clustered states,” such that oscillators in the same cluster all behaves identically, but  $z_i(t) \neq z_j(t)$  if  $i$  and  $j$  are in different clusters.

The rest of this paper is organized as follows. Section III derives the characteristic equation governing linear stability of perturbations from the  $\langle z \rangle = 0$  state. Section IV evaluates the characteristic equation for the case of a Lorentzian frequency distribution,  $g(\omega) = [\pi(1 + \omega^2)]^{-1}$ . Section V evaluates the effect of spread in  $\alpha$  on linear stability in the case of Lorentzian  $g(\omega)$  and no nonlinear frequency shift ( $\bar{\gamma} = 0$ ). Section VI evaluates the

effect of nonlinear frequency shift ( $\bar{\gamma} \neq 0$ ) on stability in the case of Lorentzian  $g(\omega)$  and no spread in  $\alpha$ . Section VII considers a flat-top frequency distribution,  $g(\omega) = U(1 - |\omega|)/2$  (where  $U(\bullet)$  denotes the unit step function) and investigates whether the qualitative behavior found in Secs. V and VI is affected by this change in the form of  $g(\omega)$ . Section VIII discusses behavior above the instability threshold for cases when there is no spread in the nonlinear parameters  $\beta$  and  $\gamma$  of (1) (as in Eq. (7)). Section IX studies stability of the corresponding nonlinear solutions in the limit of large coupling,  $\Gamma/\Gamma_c \rightarrow \infty$ , where  $\Gamma_c$  denotes the critical value of  $\Gamma$  at which the  $\langle z \rangle = 0$  state becomes unstable. A primary issue addressed in Secs. VIII and IX is the explanation of why, for sufficiently small  $\bar{\gamma}$ , macroscopic solutions become purely oscillatory with constant amplitude as  $\Gamma/\Gamma_c$  is increased (referred to as the “locked state”), and shows that multiple-clustered states with complex dynamics can occur at large  $\bar{\gamma}$ . Conclusions and further discussions are given in Sec. XI.

### III. LINEAR STABILITY OF THE $\langle z \rangle = 0$ STATE

We consider Eqs. (7) in the limit  $N \rightarrow \infty$ . In this case, there is a solution corresponding to zero value of the order parameter  $\langle z \rangle$ . For  $\langle z \rangle = 0$ , Eq. (7a) has the solutions

$$z_i = 0 \text{ for } \alpha_i < 0, \quad (10a)$$

$$z_i = \sqrt{\alpha_i} \exp\{i[(\omega_i - \bar{\gamma}\alpha_i)t + \theta_{0i}]\} \text{ for } \alpha_i > 0. \quad (10b)$$

We express the order parameter  $\langle z \rangle$  as

$$\langle z \rangle = \langle z \rangle_- + \langle z \rangle_+, \quad (11a)$$

$$\langle z \rangle_- = \frac{1}{N} \sum_{i, \alpha_i < 0} z_i, \quad (11b)$$

$$\langle z \rangle_+ = \frac{1}{N} \sum_{i, \alpha_i > 0} z_i, \quad (11c)$$

That is,  $\langle z \rangle_-$  and  $\langle z \rangle_+$  denote the contribution to the order parameter from oscillators with  $\alpha_i < 0$  and  $\alpha_i > 0$ , respectively. Note that (10a) implies  $\langle z \rangle_- = 0$ , while (10b) implies  $\langle z \rangle_+ = 0$  if  $N \rightarrow \infty$  and the angles  $\theta_{0i}$  are uniformly distributed in  $[0, 2\pi]$ . Thus, by (11a),

we see that  $\langle z \rangle = 0$  is indeed a self-consistent solution of the system (7) for  $N \rightarrow \infty$ . We now ask whether this solution is stable to small perturbations. If it is not, then the state  $\langle z \rangle = 0$  will not persist, and global collective behavior will result. We denote the perturbation of the order parameter by

$$\langle \delta z \rangle = \langle \delta z \rangle_- + \langle \delta z \rangle_+, \quad (12a)$$

$$\langle \delta z \rangle_{\pm} = \frac{1}{N} \sum_{i, \alpha_i \gtrless 0} \delta z_i, \quad (12b)$$

where  $\delta z_i$  is a perturbation from the unperturbed orbit dynamics given by Eqs. (10).

*Calculation of  $\langle \delta z \rangle_-$ .* Considering oscillator  $i$  for which  $\alpha_i < 0$ , and perturbing Eq. (7a) about  $z_i = 0$ , we obtain the linearized equation,

$$\frac{d\delta z_i}{dt} = (\alpha_i + i\omega_i)\delta z_i + \Gamma\langle \delta z \rangle. \quad (13)$$

Assuming exponential time dependence of the orbit perturbations,  $\delta z_i \sim \exp(st)$ , Eq. (13) yields

$$\delta z_i = \frac{\Gamma\langle \delta z \rangle}{(s + |\alpha_i| - i\omega)} \text{ for } \alpha_i < 0. \quad (14)$$

Thus

$$\langle \delta z \rangle_- = \Gamma\langle \delta z \rangle \int_{-\infty}^{\infty} \int_{-\infty}^0 \frac{g(\omega)h(\alpha)}{(s + |\alpha| - i\omega)} d\alpha d\omega, \quad (15)$$

where for  $N \rightarrow \infty$  we have replaced the sum over  $i$  in (11b) by integration over  $\omega$  and  $\alpha$  weighted by the pdf's  $g(\omega)$  and  $h(\alpha)$  [Eq. (6)]. Note that the  $\alpha$  integration in (15) runs from  $\alpha = -\infty$  to  $\alpha = 0$  and thus includes only those oscillators for which  $\alpha < 0$ .

*Formulation for calculating  $\langle \delta z \rangle_+$ .* We begin by re-expressing Eq. (7a) in polar form,  $z_i = \rho_i \exp(i\theta_i)$  where  $\rho_i(t)$  and  $\theta_i(t)$  are real,

$$\frac{d\rho_i}{dt} = \alpha_i\rho_i - \rho_i^3 + \Gamma \text{Re}\{e^{-i\theta}\langle z \rangle\}, \quad (16a)$$

$$\frac{d\theta_i}{dt} = \omega_i - \bar{\gamma}\rho_i^2 + \frac{\Gamma}{\rho_i} \text{Im}\{e^{-i\theta}\langle z \rangle\}, \quad (16b)$$

$$\langle z \rangle = \langle \rho e^{i\theta} \rangle. \quad (16c)$$

We now introduce a pdf for the state variables  $(\rho, \theta)$  and parameters  $(\omega, \alpha)$  which we denote by

$$f(\rho, \theta, \omega, \alpha, t).$$

Thus

$$\int_0^{2\pi} \int_0^\infty f d\rho d\theta = g(\omega)h(\alpha).$$

By conservation of the number of oscillators and Eqs. (16),  $f$  satisfies the following continuity equation,

$$\begin{aligned} \frac{\partial f}{\partial t} + \frac{\partial}{\partial \rho} \left\{ \left[ \alpha \rho - \rho^3 + \frac{\Gamma}{2} (e^{-i\theta} \langle z \rangle + e^{i\theta} \langle z \rangle^*) \right] f \right\} \\ + \frac{\partial}{\partial \theta} \left\{ \left[ \omega - \bar{\gamma} \rho^2 + \frac{\Gamma}{2i\rho} (e^{-i\theta} \langle z \rangle - e^{i\theta} \langle z \rangle^*) \right] f \right\} = 0, \end{aligned} \quad (17)$$

where

$$\langle z \rangle = \iiint \rho e^{i\theta} f d\rho d\theta d\omega d\alpha. \quad (18)$$

For  $\alpha > 0$  the time independent incoherent ( $\langle z \rangle_+ \equiv 0$ ) solution of (17) and (18) is

$$f_0 = \frac{g(\omega)h(\alpha)}{2\pi} \delta(\rho - \sqrt{\alpha}). \quad (19)$$

We now introduce a perturbation to the solution (19),

$$f = f_0 + e^{st-i\theta} \delta f + \{O.P.T.\}, \quad (20)$$

where  $\{O.P.T.\}$  denotes ‘‘other perturbation terms’’ whose  $\theta$  variation is proportional to  $\exp(in\theta)$  with  $n \neq -1$ . These other terms do not contribute to  $\langle z \rangle_+$  [see Eq. (18)] and so turn out to be of no consequence to what follows. Inserting (20) and (19) into (17) we obtain for  $\alpha > 0$

$$\begin{aligned} (s - i\omega + i\bar{\gamma}\rho^2) \delta f + \frac{\partial}{\partial \rho} [(\alpha - \rho^2) \rho \delta f] = \\ \frac{\Gamma \langle \delta z \rangle g(\omega) h(\alpha)}{4\pi} \left\{ \frac{\delta(\rho - \sqrt{\alpha})}{\sqrt{\alpha}} - \delta'(\rho - \sqrt{\alpha}) \right\}, \end{aligned} \quad (21)$$

where

$$\delta'(\rho - \sqrt{\alpha}) = \frac{d}{d\rho}\delta(\rho - \sqrt{\alpha}).$$

*Calculation of  $\langle \delta z \rangle_+$ .* We now solve (21) for  $\delta f$ . To do this we assume a solution of the form

$$\delta f = \frac{\Gamma\langle \delta z \rangle g(\omega) h(\alpha)}{4\pi} [c_1(\omega, s)\delta(\rho - \sqrt{\alpha}) + c_2(\omega, s)\delta'(\rho - \sqrt{\alpha})], \quad (22)$$

and substitute this assumed form into (21). Using the delta function identities

$$\begin{aligned} F(\rho)\delta(\rho - \sqrt{\alpha}) &= F(\sqrt{\alpha})\delta(\rho - \sqrt{\alpha}), \\ F(\rho)\delta'(\rho - \sqrt{\alpha}) &= F(\sqrt{\alpha})\delta'(\rho - \sqrt{\alpha}) - F'(\sqrt{\alpha})\delta(\rho - \sqrt{\alpha}), \end{aligned}$$

(where the second of these identities follows from differentiating the first), Eq. (21) yields

$$T_1 + T_2 = \frac{1}{\sqrt{\alpha}}\delta - \delta' \quad (23)$$

where  $\delta = \delta(\rho - \sqrt{\alpha})$ ,  $\delta' = \delta'(\rho - \sqrt{\alpha})$ ,  $T_1$  results from the first term on the left hand side of (21),

$$\begin{aligned} T_1 &= (s - i\omega + i\bar{\gamma}\rho^2)(c_1\delta + c_2\delta') \\ &= (s - i\omega + i\bar{\gamma}\alpha)(c_1\delta + c_2\delta') - 2i\bar{\gamma}\sqrt{\alpha}c_2\delta, \end{aligned}$$

and  $T_2$  results from the second term on the left hand side of (21),

$$T_2 = \frac{\partial}{\partial \rho} \{(\alpha - \rho^2)\rho(c_1\delta + c_2\delta')\} = 2\alpha c_2\delta'.$$

Separately equating coefficients of  $\delta$  and  $\delta'$  on the two sides of (23), we obtain two linear equations for the coefficients  $c_1$  and  $c_2$ . Solution of these equations yields

$$\begin{aligned} c_1 &= \frac{1}{\sqrt{\alpha}} \frac{s - i\omega + 2\alpha - i\bar{\gamma}\alpha}{s - i\omega + 2\alpha + i\bar{\gamma}\alpha} \cdot \frac{1}{s - i\omega + i\bar{\gamma}\alpha}, \\ c_2 &= -\frac{1}{s - i\omega + i\bar{\gamma}\alpha + 2\alpha}. \end{aligned}$$

Insertion of (22) with these expressions for  $c_1$  and  $c_2$  into (18) then yields  $\langle \delta z \rangle_+$ ,



$$\langle \delta z \rangle_+ = \Gamma \langle \delta z \rangle \int_{-\infty}^{+\infty} d\omega g(\omega) \left\{ \int_0^{+\infty} \frac{(s - i\omega + \alpha)h(\alpha)}{[s - i\omega + 2\alpha + i\bar{\gamma}\alpha][s - i\omega + i\bar{\gamma}\alpha]} d\alpha \right\}. \quad (24)$$

Note that the  $\alpha$  integration in (24) is only over positive  $\alpha$  (i.e., the integration runs from  $\alpha = 0$  to  $\alpha = \infty$ .)

*Equation determining  $s$ .* Inserting (15) and (24) into (12a) we obtain,

$$\Gamma^{-1} = \int_{-\infty}^{\infty} \int_0^{+\infty} \frac{(s - i\omega + \alpha)g(\omega)h(\alpha)d\alpha d\omega}{[s - i\omega + 2\alpha + i\bar{\gamma}\alpha][s - i\omega + i\bar{\gamma}\alpha]} + \int_{-\infty}^{\infty} \int_{-\infty}^0 \frac{g(\omega)h(\alpha)d\alpha d\omega}{s + |\alpha| - i\omega} \equiv D(s). \quad (25)$$

By causality, this expression for the dispersion function  $D(s)$ , as well as our previous results, Eqs. (15) and (24), for  $\langle \delta z \rangle_-$  and  $\langle \delta z \rangle_+$ , are defined with  $Re(s) > 0$ . This implies the  $\omega$ -integration contour should pass above all poles in the complex  $\omega$ -plane. We note that for  $Re(s) > 0$  the  $\omega$ -integration poles in (15), (24) and (25) all lie in the lower half  $\omega$ -plane. Since we are interested in the occurrence of instability, and instability corresponds to  $Re(s) > 0$ , the form giving  $D(s)$  by (25) is sufficient for our purposes ( $D(s)$  for  $Re(s) \leq 0$  can be obtained by analytic continuation, from the  $Re(s) > 0$  result).

#### IV. LORENTZIAN FREQUENCY DISTRIBUTION

As discussed in Sec. I, and as we will verify by the example in Sec. VII, we believe that different monotonically decreasing, continuous frequency distribution functions  $g(\omega)$  often (but not always Ref. [33]) yield similar qualitative behavior, and we, therefore, specialize here to one such  $g(\omega)$  that allows easy analytic evaluation of the integrals over  $\omega$ , namely, the case of Lorentzian  $g(\omega)$ ,

$$g(\omega) = \frac{1}{\pi} \frac{1}{\omega^2 + 1} = \frac{1}{2\pi i} \left\{ \frac{1}{\omega - i} - \frac{1}{\omega + i} \right\}, \quad (26)$$

where we have adopted a normalization of  $t, \Gamma$  and  $\alpha$  so that the half-width of  $g(\omega)$  is one ( $g(0) = 2g(1)$ ). Since  $Re(s) > 0$ , the only  $\omega$ -pole of the integrands in (25) that is located in  $Im(\omega) \geq 0$  is the one at  $\omega = i$  [see Eq. (26)]. In addition, the magnitudes of the

integrands behave like  $|\omega|^{-3}$  for large  $|\omega|$ . Thus, we can deform the  $\omega$ -integration path by shifting it upward into the complex  $\omega$ -plane, letting  $Im(\omega)$  along the path approach  $+\infty$ . The integration then yields the residue of the pole at  $\omega = i$ ,

$$D(s) = \int_0^{+\infty} \frac{(s+1+\alpha)h(\alpha)d\alpha}{[s+1+2\alpha+i\bar{\gamma}\alpha][s+1+i\bar{\gamma}\alpha]} + \int_{-\infty}^0 \frac{h(\alpha)d\alpha}{s+|\alpha|+1}. \quad (27)$$

In Sec. V we investigate conditions under which Eq. (27) predicts instability (i.e., existence of a solution to  $D(s) = \Gamma^{-1}$  with  $Re(s) > 0$ ).

## V. CONDITION FOR INSTABILITY OF THE $\langle z \rangle = 0$ STATE: THE EFFECT OF A SPREAD IN THE GROWTH RATES IN $\alpha$

In this section, we consider the case where there is no nonlinear frequency shift (i.e.,  $\bar{\gamma} = 0$ ), with  $g(\omega)$  being Lorentzian. Using a generalization of the technique in Ref. [25] (see proof of their Theorem 2), it can be shown that the solution of  $D(s) = 1/\Gamma$  is real. Thus, as we pass from stability to instability,  $s$  goes through  $s = 0$ . This results in the following general condition for instability,

$$\Gamma > \frac{1}{D(0)}, \quad (28)$$

and (27) and (28) imply that instability occurs when  $\Gamma$  exceeds the critical value  $\Gamma_c$  given by

$$\Gamma_c = \left\{ \int_0^{\infty} \frac{\alpha+1}{2\alpha+1} h(\alpha) d\alpha + \int_{-\infty}^0 \frac{1}{1-\alpha} h(\alpha) \right\}^{-1}. \quad (29)$$

As a simple reference case, we first consider (29) when there is no dispersion in  $\alpha$ ,

$$h(\alpha) = \delta(\alpha - \bar{\alpha})$$

in which case we obtain

$$\Gamma_c = \begin{cases} (2\bar{\alpha}+1)/(\bar{\alpha}+1), & \text{for } \bar{\alpha} \geq 0, \\ 1+|\bar{\alpha}|, & \text{for } \bar{\alpha} \leq 0. \end{cases} \quad (30)$$

The resulting phase diagram is given by the black line in Fig. 2. This result (with the different parametrization used in Eq. (8)) has been previously obtained in Refs. [26, 27].

Note that  $\Gamma_c \rightarrow 2$  as  $\bar{\alpha} \rightarrow +\infty$ . The value  $\Gamma_c = 2$  is the critical coupling value that applies for the Kuramoto model with a Lorentzian frequency pdf, Eq. (26). The applicability of the Kuramoto result for large  $\bar{\alpha}$  can be understood from Eq. (16a) with  $\Gamma$  neglected,  $d\rho/dt = \bar{\alpha}\rho - \rho^3$ , which when linearized about the incoherent equilibrium value,  $\rho = \sqrt{\bar{\alpha}}$ , yields  $d\delta\rho/dt = -2\bar{\alpha}\delta\rho$ . Thus perturbations from  $\rho = \sqrt{\bar{\alpha}}$  relax at the exponential rate  $2\bar{\alpha}$ , and, for large  $\bar{\alpha}$ , this rate becomes much faster than the other relevant time scale, namely, the spread in  $\omega$  (which we have normalized to 1). Hence, for  $\bar{\alpha} \gg 1$ , the oscillator amplitude is essentially frozen, and the Kuramoto oscillator description is valid. As shown in Fig. 2 and Eq. (30), when  $\bar{\alpha} \gg 1$  does not hold, the effect of amplitude dynamics is to reduce  $\Gamma_c$  (for  $\bar{\alpha} \geq 0$ ) from the Kuramoto value with the reduction increasing to a factor of 2 as  $\bar{\alpha} \rightarrow 0^+$  ( $\Gamma_c = 2$  at  $\bar{\alpha} \rightarrow +\infty$  in comparison with  $\Gamma_c = 1$  at  $\bar{\alpha} = 0$ ). An additional interesting point is that comparison of the black line in Fig. 2 with the results for the phase diagram in the case of Belousov-Zhabotinsky system of Ref. [2] (see discussion in Sect. I) shows a striking qualitative similarity between the two (e.g., see Fig. 3 of Ref. [2]).

Referring to Eq. (30) and Fig. 2, we see that there is a sharp transition in behavior as  $\bar{\alpha}$  crosses  $\bar{\alpha} = 0$ . In particular, the  $\langle z \rangle = 0$  state for  $\bar{\alpha} < 0$  results from the fact that  $z_i = 0$  for all oscillators, while for  $\bar{\alpha} > 0$  all oscillators have  $|z_i| = \sqrt{\bar{\alpha}} > 0$  and  $\langle z \rangle = 0$  results from incoherence of the individual oscillator phases. This sharp transition in behavior is reflected by the discontinuity of the derivative,  $d\Gamma_c/d\bar{\alpha}$ , at  $\bar{\alpha} = 0$ . The sharp nature of the transition at  $\bar{\alpha} = 0$  is, however, a nonphysical artifact of the assumption of no dispersion in the individual oscillator growth / damping rates used in obtaining (30). In typical physical situations, such as the experiment in Ref. [2] (see discussion in Sect. II), dispersion in  $\alpha$  is to be expected (Fig. 1). To simply illustrate its effect we consider the example where  $h(\alpha)$  is uniform within some range  $\delta\alpha$  about an average value  $\bar{\alpha}$ ,

$$h(\alpha) = (2\delta\alpha)^{-1}U(\delta\alpha - |\alpha - \bar{\alpha}|), \quad (31)$$

where  $U(x)$  denotes the unit step function;  $U(x) = 1$  for  $x \geq 0$  and  $U(x) = 0$  for  $x < 0$ . Using (31) in (29), we get for  $\bar{\alpha} > \delta\alpha$ ,

$$\Gamma_c^{-1} = \frac{1}{2\delta\alpha} \left[ \delta\alpha + \frac{1}{4} \ln \left( \frac{\bar{\alpha} + \delta\alpha + 1/2}{\bar{\alpha} - \delta\alpha + 1/2} \right) \right]; \quad (32)$$

for  $\bar{\alpha} < -\delta\alpha$ ,

$$\Gamma_c^{-1} = \frac{1}{2\delta\alpha} \ln \left( \frac{1 - \bar{\alpha} + \delta\alpha}{1 - \bar{\alpha} - \delta\alpha} \right); \quad (33)$$

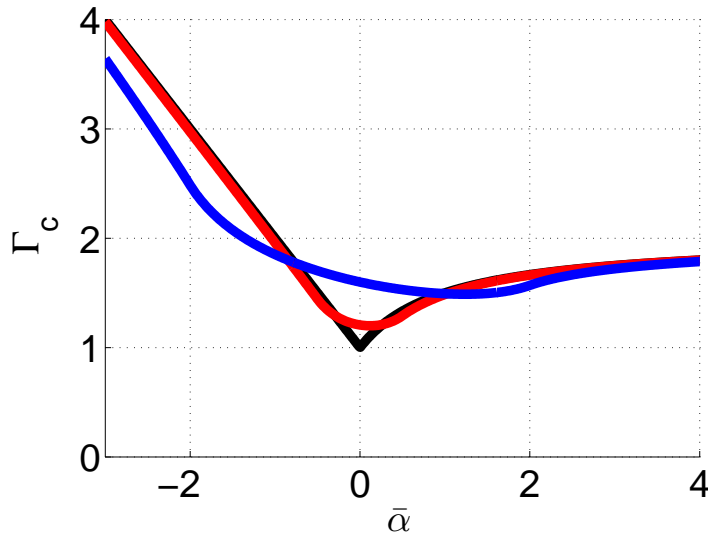


FIG. 2: (Color online) The effect of dispersion in  $\alpha$  ( $\bar{\gamma} = 0$ ) with a Lorentzian  $g(\omega)$ . Stability/Instability regions of  $\Gamma - \bar{\alpha}$  space for several different values of spread  $\delta\alpha$  in the linear growth parameter  $\alpha$  with mean  $\bar{\alpha}$  [Legend: Black line ( $\delta\alpha = 0$ ), red line ( $\delta\alpha = 0.5$ ), blue line ( $\delta\alpha = 2$ )].

and for  $|\bar{\alpha}| < \delta\alpha$ ,

$$\Gamma_c^{-1} = \frac{1}{2\delta\alpha} \left[ \frac{\bar{\alpha} + \delta\alpha}{2} + \ln(1 - \bar{\alpha} + \delta\alpha) + \frac{1}{4} \ln(1 + 2\bar{\alpha} + 2\delta\alpha) \right]. \quad (34)$$

As the dispersion in  $\alpha$ ,  $\delta\alpha$ , approaches zero, (31) becomes a delta function, and Eqs. (32)-(34) reduce to (30). The other two lines in Fig. 2 show the phase diagram from Eqs. (32)-(34) for two more values of  $\delta\alpha$ . For  $\delta\alpha > 0$  the discontinuity in  $d\Gamma_c/d\bar{\alpha}$  (which occurs for  $\delta\alpha = 0$  at  $\bar{\alpha} = 0$ ) is removed by dispersion in  $\alpha$ , and the sharp transition that occurs at  $\bar{\alpha} = 0$  (black line in Fig. 2) is now smoothed out [34]. Further, it is also noticed that the minimum of  $\Gamma_c$  rises and shifts from  $\bar{\alpha} = 0$  when  $\delta\alpha = 0$  to  $\bar{\alpha} > 0$  when  $\delta\alpha > 0$ .

## VI. CONDITION FOR INSTABILITY OF THE $\langle z \rangle = 0$ STATE: THE EFFECT OF A NONLINEAR FREQUENCY SHIFT

We now address the effect of nonlinear frequency shift,  $\bar{\gamma} \neq 0$ , and we consider the simple case of no dispersion in  $\alpha$ ,  $h(\alpha) = \delta(\alpha - \bar{\alpha})$  again for the case of Lorentzian  $g(\omega)$ . We note from Eq. (7), if the distribution of  $\omega_i$  values is symmetric, then positive and negative values of  $\bar{\gamma}$  are equivalent ( $z_i \rightarrow z_i^*$ ). Thus, we consider  $\bar{\gamma} > 0$  only. As is evident from Eq. (27),

$\bar{\gamma}$  has no effect on the linear theory for  $\bar{\alpha} < 0$ , and, consequently, the result for  $\Gamma_c$  given by Eq. (30) still applies for  $\bar{\alpha} \leq 0$ . For  $\bar{\alpha} > 0$ , however, the effect of a nonlinear frequency shift can be substantial. Equation (27) for  $h(\alpha) = \delta(\alpha - \bar{\alpha})$ ,  $\bar{\alpha} > 0$  gives

$$\Gamma^{-1} = D(s) = \frac{s + 1 + \bar{\alpha}}{(s + 1 + 2\bar{\alpha} + i\bar{\gamma}\bar{\alpha})(s + 1 + i\bar{\gamma}\bar{\alpha})}, \quad (35)$$

which yields a quadratic equation for  $s$ , solution of which can be used to obtain stability boundary curves in  $\Gamma - \bar{\alpha}$  space. At the transition point,  $Re(s)$  goes through zero. Substituting  $s = i\Omega$  into Eq. (35) and separating the real and imaginary parts,  $\Gamma_c$  and  $\Omega$  are then given by the solution of the following pair of equations

$$1 - \Omega^2 + 2\bar{\alpha}(1 - \bar{\gamma}\Omega) - \bar{\alpha}^2\bar{\gamma}^2 = \Gamma_c(1 + \bar{\alpha}), \quad (36a)$$

$$2(1 + \bar{\alpha})(\Omega + \bar{\alpha}\bar{\gamma}) = \Gamma_c\Omega. \quad (36b)$$

When  $\bar{\gamma} = 0$  (note  $\Omega = 0$  for this case), the solution for the critical coupling strength of (36) is given by

$$\Gamma_{c0} = \frac{1 + 2\bar{\alpha}}{1 + \bar{\alpha}}, \quad (37)$$

by which (36a) can be rearranged to give

$$\Gamma_c = \Gamma_{c0} - \frac{(\Omega + \bar{\alpha}\bar{\gamma})^2}{1 + \bar{\alpha}}, \quad (38)$$

which shows that the effect of  $\bar{\gamma}$  is always to decrease  $\Gamma_c$ . Figure 3 shows the values of  $\Gamma_c$  as a function of  $\bar{\alpha}$  for several different values of  $\bar{\gamma}$  ( $\bar{\gamma} = 0$  plotted in black,  $\bar{\gamma} = 2$  plotted in red, and  $\bar{\gamma} = 4$  plotted in blue). By solving for  $\Omega$  in (36b) and substituting it back in (36a), we obtain

$$\Gamma_c = \Gamma_{c0} - \frac{1}{1 + \bar{\alpha}} \left[ \frac{\bar{\alpha}\bar{\gamma}\Gamma_c}{\Gamma_c - 2(1 + \bar{\alpha})} \right]^2. \quad (39)$$

Equation (39) shows that  $\Gamma_c \rightarrow 2$  as  $\bar{\alpha} \rightarrow +\infty$ . As seen in Fig. 3, increasing  $\bar{\gamma}$  eventually moves the minimum of  $\Gamma_c$  below one and shifts the location of the minimum into  $\bar{\alpha} > 0$ .

## VII. THE EFFECT OF THE FREQUENCY DISTRIBUTION FUNCTION

In Secs. V and VI we consider the effect of a spread in  $\alpha$  and of a nonlinear frequency shift for the illustrative case of a Lorentzian distribution function of the oscillator natural

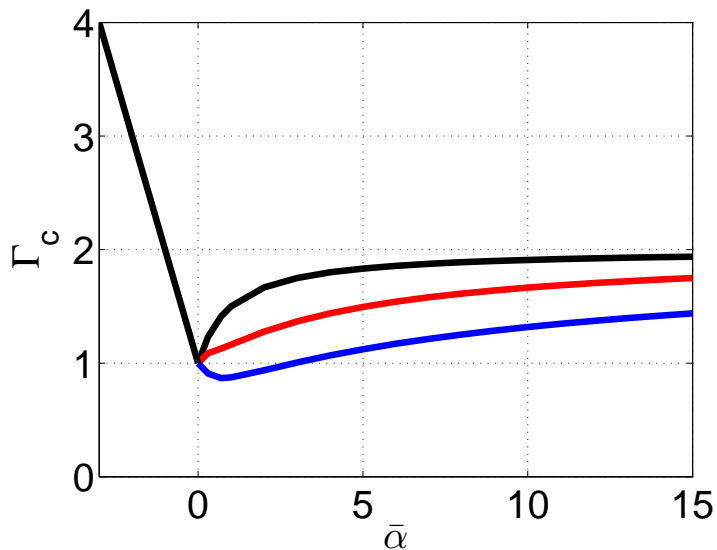


FIG. 3: (Color online) Stability / Instability regions of  $\Gamma - \bar{\alpha}$  space for several different values of the nonlinear frequency shift parameter  $\bar{\gamma}$  [Legend: Black line ( $\bar{\gamma} = 0$ ), red line ( $\bar{\gamma} = 2$ ), blue line ( $\bar{\gamma} = 4$ )]. Notice that the three lines coincide when  $\bar{\alpha} < 0$ .

frequencies, Eq. (26). We now ask how might these results be altered if a different frequency distribution were used. We note that the Lorentzian decays rather slowly for large  $\omega$ ,  $g(\omega) \sim \omega^{-2}$ . Thus to test dependence on the form of  $g(\omega)$ , we will examine another distribution function which is very different from the Lorentzian, in that it has a sharp cutoff to  $g(\omega) = 0$  as  $\omega$  increases. In particular, we will consider a “flat-top” distribution, that is uniform in  $-1 \leq \omega \leq 1$  and zero otherwise,

$$g(\omega) = \frac{1}{2}U(1 - |\omega|), \quad (40)$$

where  $U(x)$  is the unit step function. In spite the qualitatively different large  $|\omega|$  behavior of the Lorentzian and the flat-top  $g(\omega)$  distributions, we will find that the resulting stability conditions show qualitatively similar behavior.

The calculation of  $\Gamma_c$  with  $g(\omega)$  given by (40) is done by using (25) (see the Appendix). In Fig. 4 we show the dependence of  $\Gamma_c$  on  $\bar{\alpha}$  for several different values of  $\delta\alpha$ , where  $h(\alpha)$  is given by (31) and  $\bar{\gamma} = 0$  for all oscillators. A comparison between Fig. 4 and Fig. 2 reveals remarkably similar dependence, apart from a difference in the vertical scale due to different functional dependence of  $g(\omega)$  [35]. Next, we consider the dependence of  $\Gamma_c$  on  $\bar{\gamma}$  when  $h(\alpha) = \delta(\alpha - \bar{\alpha})$  with  $g(\omega)$  given by (40). Figure 5 shows the dependence of  $\Gamma_c$  on  $\bar{\alpha}$

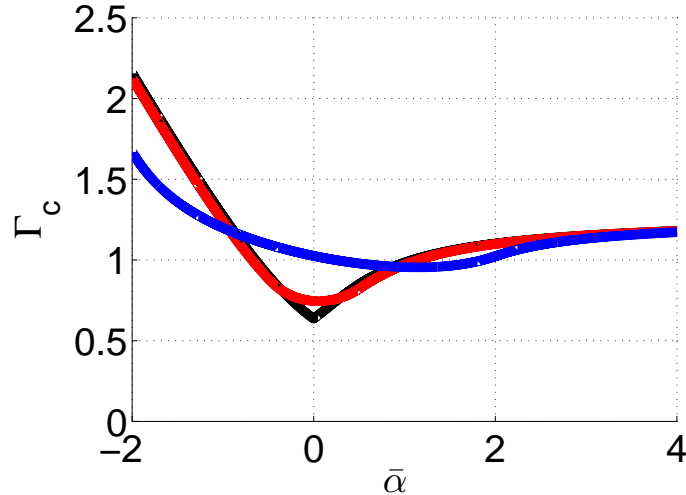


FIG. 4: (Color online) The effect of dispersion in  $\alpha$  with a uniformly distributed  $g(\omega)$ , Eq. (40). Stability/Instability regions of  $\Gamma - \bar{\alpha}$  space for several different values of spread  $\delta\alpha$  in the linear growth parameter  $\alpha$  with mean  $\bar{\alpha}$  [Legend: Black line ( $\delta\alpha = 0$ ), red line ( $\delta\alpha = 0.5$ ), blue line ( $\delta\alpha = 2.0$ )].

for several different values of  $\bar{\gamma}$ . The black line shows the result when  $\bar{\gamma} = 0$ , which is the same black line in Fig. 4. The other two lines are obtained by numerically solving Eq. (A7) in the Appendix when  $\bar{\gamma} \neq 0$ . In comparison with Fig. 3, we see similar dependence in that, as  $\bar{\gamma}$  increases,  $\Gamma_c$  decreases.

### VIII. NONLINEAR PHENOMENA ABOVE THE INSTABILITY THRESHOLD WITH FINITE $\alpha$ -SPREAD AND NONLINEAR FREQUENCY SHIFT

In the previous sections, we calculated the critical coupling strength  $\Gamma_c$  marking the onset of instability of the quiescent state ( $\langle z \rangle = 0$ ). Above the critical value  $\Gamma_c$ , we find that Landau-Stuart oscillator networks exhibit a rich variety of collective behavior. We now briefly review past work on the nonlinear behavior found above the instability threshold.

Matthews et al. [27] studied nonlinear collective behavior in the special case that  $\alpha_j = 1$  and  $\gamma_j = 0$  for all oscillators ( $j = 1, 2, \dots, N$ ), and  $g(\omega)$  takes on several different functional forms. An important observation in that paper is that the system behavior can be quite complicated for a range of  $\Gamma$  not too far above  $\Gamma_c$ . For example, they found period doubling

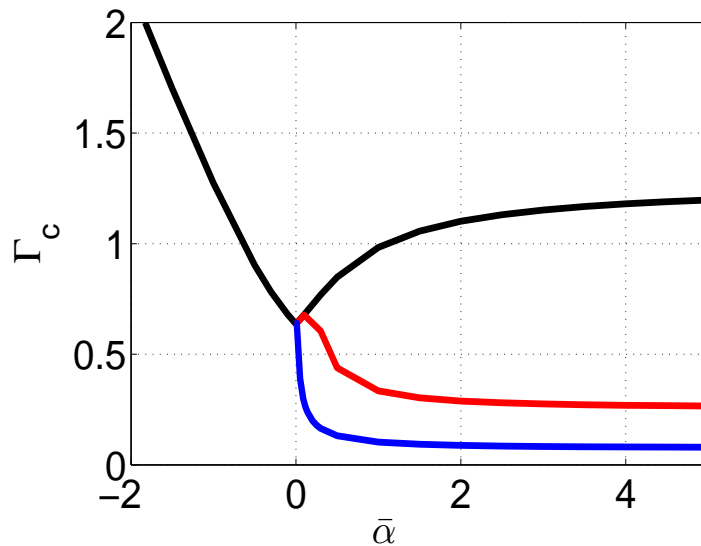


FIG. 5: (Color online) Stability / Instability regions of  $\Gamma - \bar{\alpha}$  space for several different values of the nonlinear frequency shift parameter  $\bar{\gamma}$  [Legend: Black line ( $\bar{\gamma} = 0$ ), red line ( $\bar{\gamma} = 2$ ), blue line ( $\bar{\gamma} = 4$ )]. Notice that the three lines coincide when  $\bar{\alpha} < 0$ .

cascades to chaos, large amplitude oscillations, quasiperiodicity, and hysteretic behavior close to the boundaries between different macroscopic states. However, when  $\Gamma$  is sufficiently far from  $\Gamma_c$ , the system was always found to settle into a steady oscillatory state,  $\langle z \rangle = \text{constant} \times \exp(i\Omega t)$  for some constant  $\Omega$ . We refer to this as a “locked state,” which we define as a solution of (17) and (18) for which the oscillator distribution  $f$  has dependence on  $(\rho, \theta, t)$  of the form  $f = f(\rho, \theta - \Omega t)$ ; i.e., the entire distribution rigidly rotates about the origin of the complex  $z$ -plane with the uniform rotation rate  $\Omega$ .

When the nonlinear frequency shift parameter  $\bar{\gamma}$  is nonzero [37–40], the system can exhibit additional types of complicated coherent behavior. For example, Refs. [37–41] studied systems closely related to Eq. (7), but with homogeneous parameters. An important feature found in those references is the tendency for the system to form clusters (a “cluster” in this case is defined as a group of oscillators which behave identically). Further, depending on parameter values and on initial conditions, the systems can form cluster states of varying sizes. In Refs. [38] and [39], the authors also found chaotic behavior.

We emphasize the finding of Ref. [27] that, for zero nonlinear frequency shift  $\gamma_i \equiv 0$  the system always goes to a locked state attractor when  $\Gamma$  is sufficiently large. Consistent with



this, we find that when we include spreads in  $\alpha$ , and  $\omega$ , and simultaneously allow  $\beta_j = \bar{\beta} \neq 0$  and  $\gamma_j = \bar{\gamma} \neq 0$ , it is the case that, as  $\Gamma$  is increased, there is always a locked state that the system may settle into. Furthermore, we analytically prove that this locked state is the only large  $\Gamma$  attractor (as in [27] which has  $\gamma_i \equiv 0$ ) *provided* that the nonlinear frequency shift  $\bar{\gamma}$  is not too large, but we also find that other coexisting attractors may be present if  $\bar{\gamma}$  is large enough. This will be discussed further in Secs. IX and X. As an example of a locked state, Fig. 6 shows snapshots of the long-time asymptotic distributions of the oscillator  $z$ -values obtained from numerical simulations of Eq. (7) with  $g(\omega)$  given by (40),  $N = 50000$ ,  $h(\alpha)$  given by (31),  $\bar{\alpha} = 0.5$ ,  $\delta\alpha = 1.0$ ,  $\bar{\gamma} = 0.5$  (corresponding to  $\Gamma_c = 0.89$ ), for successively larger values of  $\Gamma/\Gamma_c$ , all of which are large enough that a locked state is achieved (Fig. 6(a):  $\Gamma/\Gamma_c = 2$ , Fig. 6(b):  $\Gamma/\Gamma_c = 10$ , Fig. 6(c):  $\Gamma/\Gamma_c = 100$ ). Note that, as appropriate for a locked state, as time increases, these snapshots rotate uniformly about the origin at a fixed angular rate  $\Omega$ .

We see in Fig. 6(a) that the distribution has finite spreads in both the magnitude and phase of  $z$ . Examination of the solution shows that oscillators with smaller (larger) natural frequencies  $\omega$  tend to occur on the clockwise (counterclockwise) side of the distribution, while larger (smaller)  $\alpha$  tend to occur at larger (smaller)  $|z|$  for fixed argument of  $z$ . Previous works (e.g., [27]) did not consider a distribution of  $\alpha$  and consequently did not find a spread in  $|z|$  at constant argument of  $z$  (i.e., the oscillators are distributed along a curve in the complex  $z$ -plane). Comparing Figs. 6(a), 6(b) and 6(c), we see that the spread in  $z/|\langle z \rangle|$  becomes smaller and smaller as  $\Gamma/\Gamma_c$  increases. In fact, we argue in Sec. IX below that one of the stationary states of this system is when this spread goes to zero as  $\Gamma/\Gamma_c \rightarrow \infty$  (note the greatly magnified scale for Fig. 6(c)). Note that the oscillators in Fig. 6 are contained within a *single* region, and we subsequently refer to such states as *single-cluster* locked states.

Figure 7 illustrates an example of the occurrence and evolution of a non-locked dynamical attractor at lower  $\Gamma/\Gamma_c$  with other parameters the same as those in Fig. 6. In particular, Fig. 7 shows  $|\langle z \rangle|$  (top panel) and  $\text{Re}\langle z \rangle$  (bottom panel) versus time, after the system has settled into an attractor for  $\Gamma/\Gamma_c = 1.07$ . (Note that for a locked state,  $|\langle z \rangle|$  is constant, and  $\text{Re}\langle z \rangle$  varies sinusoidally in time.)

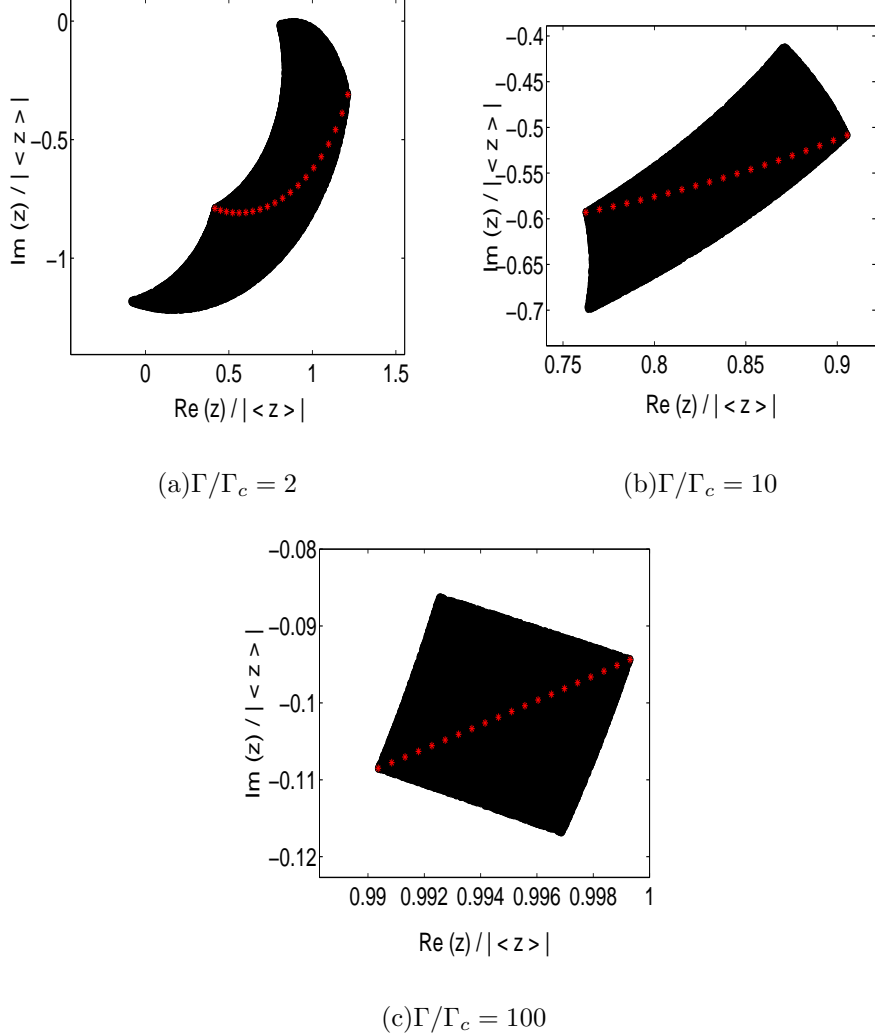


FIG. 6: (Color online) Locations of 50000 oscillators (black) in locked states with different  $\Gamma/\Gamma_c$ . Twenty oscillators (red cross) of parameter values evenly spaced simultaneously in  $(\alpha, \omega) \in [-0.5, 1.5] \times [-1, 1]$  are highlighted, i.e., the oscillator with  $(\alpha, \omega) = (-0.5, -1)$  is located at the minimum radius position, and the oscillator with  $(\alpha, \omega) = (1.5, 1)$  is located at the maximum radius position, and other oscillators of intermediate parameter values are distributed in between ( $N = 50000$ ,  $\bar{\alpha} = 0.5$ ,  $\delta\alpha = 1.0$ ,  $\bar{\gamma} = 0.5$ ; random initial conditions).

### IX. LARGE COUPLED LANDAU-STUART OSCILLATOR NETWORKS IN THE STRONG COUPLING LIMIT: SINGLE-CLUSTER LOCKED STATES

In what follows, as in all other previous references (except for the weak “coupling limit” treatment in Ref. [36]), we consider the case where there is no spread in the nonlinear

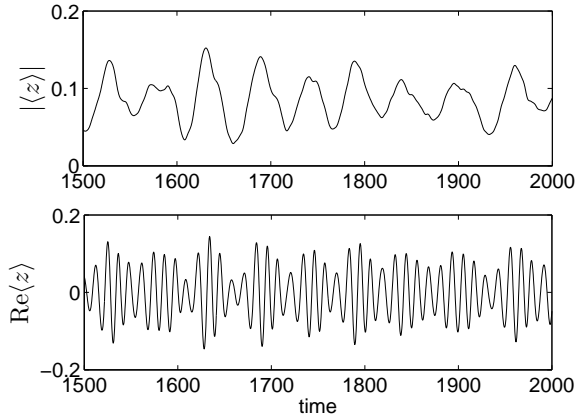


FIG. 7: Time evolution of  $|\langle z \rangle|$  (top panel) and  $\text{Re}\langle z \rangle$  (bottom panel) for a system of 500,000 oscillators (Parameters:  $\bar{\alpha} = 0.5$ ,  $\delta\alpha = 1.0$ ,  $\bar{\gamma} = 0.5$ ,  $\Gamma/\Gamma_c = 1.07$ ; random initial conditions.)

coefficients ( $\gamma_j = \bar{\gamma}$  and  $\beta_j = 1$  for all  $j$ ). In this section we ask why the single-cluster locked state is an attractor for large enough  $\Gamma$ .

In order to analytically show that a single-cluster locked state attractor must exist for homogeneous nonlinearity parameters  $\gamma_j \equiv \bar{\gamma}$  and  $\beta_j \equiv 1$  at sufficiently large  $\Gamma/\Gamma_c$ , we now consider very large  $\Gamma/\Gamma_c$  approximated by taking the limit  $\Gamma/\Gamma_c \rightarrow \infty$ . In particular, using this limit, we will show the existence of a simple single-cluster locked state and we will demonstrate that it is stable. In Sec. X we will show that the single-cluster locked state is the only attractor of the system if  $\bar{\gamma}$  is not too large, but that, when  $\bar{\gamma}$  is larger, there can be other coexisting attractors of various types composed of multiple clusters.

When  $\Gamma \gg \alpha_j, \omega_j$  for all  $j$ , system (7) reduces to

$$\frac{dz_j}{dt} = -(1 + i\bar{\gamma})|z_j|^2 z_j + \Gamma \langle z \rangle. \quad (41)$$

Here we have assumed that  $|z_j| \gg 1$  in the  $\Gamma \rightarrow \infty$  limit. This will be subsequently verified. Alternatively, if the  $\omega_j$  are uniform,  $\omega_j = \omega$ , and  $\Gamma \gg \alpha_j$ , even if  $\Gamma \gg \omega$  does not apply, we can still obtain Eq.(41) via elimination of  $\omega$  through the transformation  $z_j \rightarrow z_j e^{i\omega t}$ . Thus, in this limit, the dynamics is determined by the coupling to other oscillators and the nonlinear characteristics of the individual oscillators, rather than by the linear properties of the individual oscillators. This is consistent with our numerical tests in Fig. 6, which suggests that as  $\Gamma/\Gamma_c \rightarrow \infty$ , the distribution of oscillators approaches that of a system of homogeneous parameter values, with the effects of spreads due to  $\alpha$  and  $\omega$  going away (see

Fig. 6(c)). We now divide Eq.(41) by  $\Gamma$ , and redefine variables as

$$\hat{z}_j = \frac{z_j}{\sqrt{\Gamma}}, \quad (42a)$$

$$\hat{t} = \Gamma t. \quad (42b)$$

Thus, each term in Eq. (41) scales as  $\Gamma^{3/2}$  justifying the neglect of the other terms in Eq. (7). Equations (41) become

$$\frac{d\hat{z}_j}{d\hat{t}} = -(1 + i\bar{\gamma})|\hat{z}_j|^2\hat{z}_j + \frac{1}{N} \sum_{k=1}^N \hat{z}_k, \quad (43)$$

Making the single-cluster locked state ansatz  $\hat{z}_j = \rho(\hat{t}) \exp[i\theta(\hat{t})]$  gives

$$\frac{d\rho}{d\hat{t}} = \rho(1 - \rho^2), \quad (44a)$$

$$\frac{d\theta}{d\hat{t}} = -\bar{\gamma}\rho^2. \quad (44b)$$

This yields the time asymptotic attracting solution,

$$\hat{z}_0(\hat{t}) = e^{-i\bar{\gamma}\hat{t}}. \quad (45)$$

To analyze the stability of (45), we perturb  $\hat{z}_0$  to  $\hat{z}_0 + e^{-i\bar{\gamma}\hat{t}}\delta\hat{z}_j$ . From (43), the dynamics of  $\delta\hat{z}_j$  is governed by

$$\frac{d}{d\hat{t}}\delta\hat{z}_j = (-1 - i\bar{\gamma})(\delta\hat{z}_j + \delta\hat{z}_j^*) - \delta\hat{z}_j + \frac{1}{N} \sum_k \delta\hat{z}_k. \quad (46)$$

where \* denotes complex conjugation. Similarly, we have

$$\frac{d}{d\hat{t}}\delta\hat{z}_j^* = (-1 + i\bar{\gamma})(\delta\hat{z}_j + \delta\hat{z}_j^*) - \delta\hat{z}_j^* + \frac{1}{N} \sum_k \delta\hat{z}_k^*. \quad (47)$$

Equations (46) and (47) can be regarded as two independent equations for  $\delta\hat{z}_j$  and  $\delta\hat{z}_j^*$  respectively. To study the stability properties of  $\delta\hat{z}_j$  and  $\delta\hat{z}_j^*$ , consider  $\delta\hat{z}_j \sim \delta\hat{Z}_j(s)e^{s\hat{t}}$  and  $\delta\hat{z}_j^* \sim \delta\hat{Z}_j^*(s)e^{s\hat{t}}$ , for which Eqs. (46) and (47) give

$$(s + 2 + i\bar{\gamma})\delta\hat{Z}_j + (1 + i\bar{\gamma})\delta\hat{Z}_j^* - \langle\delta\hat{Z}\rangle = 0, \quad (48a)$$

$$(s + 2 - i\bar{\gamma})\delta\hat{Z}_j^* + (1 - i\bar{\gamma})\delta\hat{Z}_j - \langle\delta\hat{Z}^*\rangle = 0, \quad (48b)$$

where  $\langle \delta \hat{Z} \rangle = N^{-1} \sum_k \delta \hat{Z}_k$ ,  $\langle \delta \hat{Z}^* \rangle = N^{-1} \sum_k \delta \hat{Z}_k^*$ . Summing over  $j$  we obtain

$$\Upsilon \begin{bmatrix} \langle \delta \hat{Z} \rangle \\ \langle \delta \hat{Z}^* \rangle \end{bmatrix} = 0, \quad (49)$$

where

$$\Upsilon \equiv \begin{bmatrix} (s+1+i\bar{\gamma}) & (1+i\bar{\gamma}) \\ (1-i\bar{\gamma}) & (s+1-i\bar{\gamma}) \end{bmatrix}. \quad (50)$$

Equation (49) implies that either (i)  $\det \Upsilon = 0$ , or (ii)  $\langle \delta \hat{Z} \rangle = \langle \delta \hat{Z}^* \rangle = 0$ . Possibility (i) gives  $s(s+2) = 0$ , yielding  $s = 0$  and  $s = -2$ . Physically, the neutrally stable root,  $s = 0$ , corresponds to a uniform, rigid rotation of the phases of all the  $\hat{Z}_j$ . If possibility (ii) applies, Eqs. (48a) and (48b) become

$$\Psi \begin{bmatrix} \delta \hat{Z}_j \\ \delta \hat{Z}_j^* \end{bmatrix} = 0, \quad (51)$$

where

$$\Psi \equiv \begin{bmatrix} (s+2+i\bar{\gamma}) & (1+i\bar{\gamma}) \\ (1-i\bar{\gamma}) & (s+2-i\bar{\gamma}) \end{bmatrix}. \quad (52)$$

Since  $\det \Psi = (s+1)(s+3)$ , we obtain two additional roots  $s = -1$  and  $s = -3$ . Because the allowed perturbations in case (ii) are restricted to lie in the  $2(N-1)$  dimensional space specified by the two constraints,  $\langle \delta \hat{Z} \rangle = 0$  and  $\langle \delta \hat{Z}^* \rangle = 0$ , the multiplicity of each of the roots  $s = -1$  and  $s = -3$  is  $N-1$ . Since there is no root with  $Re(s) > 0$ , the equilibrium is stable. Hence, the single-cluster locked state is stable.

## X. LARGE COUPLED LANDAU-STUART OSCILLATOR NETWORKS IN THE STRONG COUPLING LIMIT: CLUSTER STATES

### A. Regime of global attraction for the single-cluster locked state

In Sec. VIII we numerically suggest the tendency of system (43) to form a single-cluster locked state when  $\Gamma$  is sufficiently large, and in Sec. IX we have shown that such an attractor always exists at large  $\Gamma$ . In this section, we give a sufficient condition for this state to be

the *only* attractor of the system. Consider any two oscillators,  $m$  and  $n$ , in (43). Let

$$\bar{\hat{z}} = \frac{\hat{z}_m + \hat{z}_n}{2}, \quad (53a)$$

$$\delta = \frac{\hat{z}_m - \hat{z}_n}{2}. \quad (53b)$$

Then the dynamical equation for the separation between the two oscillators,  $\delta$ , can be immediately derived from Eq. (43) as

$$\frac{d}{dt}\delta = -(1 + i\bar{\gamma}) (2|\bar{\hat{z}}|^2\delta + \delta^*\bar{\hat{z}}^2 + |\delta|^2\delta). \quad (54)$$

Letting  $\delta = |\delta|e^{i\nu_1}$  and  $\bar{\hat{z}} = |\bar{\hat{z}}|e^{i\nu_2}$ , substitution into (54) yields

$$\frac{d}{dt}|\delta| = -|\bar{\hat{z}}|^2|\delta|[2 + \cos(\nu_3) + \bar{\gamma}\sin(\nu_3)] - |\delta|^3, \quad (55)$$

where  $\nu_3 = 2(\nu_1 - \nu_2)$ . The trigonometric terms on the right hand side of Eq. (55) can be combined, giving

$$\frac{d}{dt}|\delta| = -|\bar{\hat{z}}|^2|\delta|[2 + \sqrt{1 + \bar{\gamma}^2}\cos(\nu_4 - \nu_3)] - |\delta|^3, \quad (56)$$

where  $\nu_4$  is determined by the conditions  $\cos(\nu_4) = 1/\sqrt{1 + \bar{\gamma}^2}$  and  $\sin(\nu_4) = \bar{\gamma}/\sqrt{1 + \bar{\gamma}^2}$ . From Eq. (56), we see that  $d|\delta|/dt < 0$  if  $2 > \sqrt{1 + \bar{\gamma}^2}$ , or equivalently  $\bar{\gamma} < \sqrt{3}$ . Thus, if  $\bar{\gamma} < \sqrt{3}$ , the attractor of system (43) must occur as a single-cluster, and, as shown in Sec. IX, a single-cluster attractor must be a locked state (45). However, we shall soon see that if  $\bar{\gamma} > \sqrt{3}$ , then Eq. (43) has the possibility of attracting solutions other than the single-cluster locked state. This technique [Eqs. (53)-(56)] can also be employed for related problems such as when the coupling is complex,  $\Gamma \rightarrow \Gamma e^{i\chi}$ , or when the coupling is in the form in Eq. (8).

## B. Cluster States

We now wish to investigate the possible existence of attracting states for (43) composed of  $C \geq 2$  clusters, where each cluster is labeled by a subscript  $c = 1, 2, \dots, C$ . Each cluster  $c$  has  $N_c$  oscillators in identical states  $Z_c$ , such that if oscillators  $i$  and  $j$  are in cluster  $c$ , then  $\hat{z}_i = \hat{z}_j = Z_c$ , and  $N_1 + N_2 + \dots + N_C = N$ . Letting  $\xi_c = N_c/N$  be the fraction of oscillators in cluster  $c$ , we have that

$$\langle Z \rangle = \xi_1 Z_1 + \cdots + \xi_C Z_C, \quad (57)$$

and that Eq. (43) reduces to  $C$  equations for the  $C$  complex cluster variables  $Z_c$  ( $c = 1, 2, \dots, C$ ),

$$\frac{dZ_c}{dt} = -(1 + i\bar{\gamma})|Z_c|^2 Z_c + \sum_{c=1}^C \xi_c Z_c. \quad (58)$$

Two questions pertaining to such cluster states are (i) what are the attractors of (58), and (ii) given an attractor of (58), are the clusters internally stable? Question (ii) asks whether, if we consider oscillators in cluster  $c$  and individually independently perturb each of them from their common value  $Z_c$ , do they relax back to a common value? (This question was considered for the one-cluster locked state in Sec. IX.)

The question of the existence of cluster state attractors is a general one applicable to any large system of identical dynamical units that are coupled via a global field (e.g., in our case  $\langle Z \rangle$ ). In particular, this type of consideration was introduced by Kaneko who considered coupled maps [42, 43].

In our numerical experiments we have always found that, at long time, the solutions of (43) settles into a finite number of clusters  $Z_c(t)$ . We caution that this does not necessarily mean that attractors of (43) always occur in clusters, but rather that we have so far not found non-clustered long-time states. References [37]-[40] consider a globally coupled Landau-Stuart system with *homogeneous* parameters across all oscillators (our (43) is a special case) and find both clustered state attractors and “scattered state” attractors, where by “scattered states” they mean that, at any given time, no two oscillators have exactly the same state. We, however, have not seen scattered state attractors, and we conjecture that they do not exist for (43). Along these lines, we now show a partial result implying that scattered states cannot have scattering that is *over an area* in the  $z$ -plane. That is, in the limit  $N \rightarrow \infty$  the distribution function  $f$  appearing in (17) must be singular in the sense that it is concentrated on a set of zero Lebesgue measure in  $z$ -space, equivalently  $(\rho, \theta)$  space. Examples of zero Lebesgue measure sets are a set of distinct points (like our clusters), a curve, or a fractal set of dimension between one and two. Indeed the scattered states seen in the figures of the previous references [37]-[40] (e.g., Fig. 1 of Ref. [40]) appear to our eye to be either fractal distributions with dimension near one or distributed along a convoluted curve (based on

Ref. [44], we suspect that the first of these alternatives applies). The demonstration that  $f$  must be singular follows simply from (17) by introducing  $F = f/\rho$  and rewriting (17) in the form

$$\frac{d}{dt}F = \frac{\partial}{\partial t}F + \dot{\rho}\frac{\partial}{\partial\rho}F + \dot{\theta}\frac{\partial}{\partial\theta}F = 4\rho^2F, \quad (59)$$

where  $\dot{\rho}$  and  $\dot{\theta}$  are the two quantities in (17) appearing within the square brackets with the linear oscillator parameters,  $\alpha$  and  $\omega$ , set to zero [to correspond to (43)]. Note too that  $F = F(\rho, \theta, t)$ ; in particular, unlike our more general set-up, Eq. (17),  $F$  does not incorporate distribution in parameters as we have fixed  $\alpha$  and  $\omega$  at zero. According to (59), following the characteristics,  $d\rho/dt = \dot{\rho}$ ,  $d\theta/dt = \dot{\theta}$ , of the partial differential equation (17) with  $\alpha = \omega = 0$ ,  $F$  increases continually at the exponential rate  $4\rho^2$ . Thus, since  $\int f d\rho d\theta = \int F \rho d\rho d\theta = 1$ , we immediately conclude that in the long time limit,  $F$  and hence  $f$  must concentrate on a set of zero area (zero Lebesgue measure) in  $(\rho, \theta)$  space. Proof that our system (43) does or does not always yield cluster state attractors remains an open problem.

### C. Two-cluster states

For  $C = 2$ , Eq. (58) yields

$$\frac{dZ_1}{d\hat{t}} = -(1 + i\bar{\gamma})|Z_1|^2 Z_1 + \xi_1 Z_1 + \xi_2 Z_2, \quad (60a)$$

$$\frac{dZ_2}{d\hat{t}} = -(1 + i\bar{\gamma})|Z_2|^2 Z_2 + \xi_1 Z_1 + \xi_2 Z_2. \quad (60b)$$

Letting  $Z_1 = \tilde{\rho}_1 e^{i\tilde{\theta}_1}$  and  $Z_2 = \tilde{\rho}_2 e^{i\tilde{\theta}_2}$ , and defining the relative phase difference  $\tilde{\phi} = \tilde{\theta}_1 - \tilde{\theta}_2$ , Eq. (60) yields three real equations,

$$\frac{d\tilde{\rho}_1}{d\hat{t}} = \tilde{\rho}_1(\xi_1 - \tilde{\rho}_1^2) + \xi_2 \tilde{\rho}_2 \cos(\tilde{\phi}), \quad (61a)$$

$$\frac{d\tilde{\rho}_2}{d\hat{t}} = \tilde{\rho}_2(\xi_2 - \tilde{\rho}_2^2) + \xi_1 \tilde{\rho}_1 \cos(\tilde{\phi}), \quad (61b)$$

$$\frac{d\tilde{\phi}}{d\hat{t}} = -\bar{\gamma}(\tilde{\rho}_1^2 - \tilde{\rho}_2^2) - \sin(\tilde{\phi}) \left[ \xi_2 \frac{\tilde{\rho}_2}{\tilde{\rho}_1} + \xi_1 \frac{\tilde{\rho}_1}{\tilde{\rho}_2} \right]. \quad (61c)$$



Note that  $\tilde{\rho}_1 = \tilde{\rho}_2 = 1$  and  $\tilde{\phi} = 0$  is a solution of these equations and corresponds to the single-cluster locked state. We want to obtain two-cluster solutions ( $Z_1 \neq Z_2$ ). Although we cannot rule out chaotic or two-frequency quasiperiodic two-cluster solutions of Eq. (61), so far our numerical investigations of Eqs. (61) have only found fixed point attractors (i.e., uniformly rotating two-cluster locked states) and periodic attractors. In the next two subsections we discuss the fixed point solutions (Sec. XC 1) and the periodic solutions (Sec. XC 2).

1. *Two-cluster locked states (fixed point solutions of Eq. (61))*

When the time derivatives in Eq. (61) are all zero, the solutions give locked two-cluster fixed point solutions. By setting  $d/dt = 0$ ,  $x = \tilde{\rho}_1^2$  and  $y = \tilde{\rho}_2^2$ , elimination of  $\cos(\tilde{\phi})$  between Eqs. (61a) and (61b) gives

$$\xi_1 \left( x - \frac{\xi_1}{2} \right)^2 - \xi_2 \left( y - \frac{\xi_2}{2} \right) = \frac{1}{4}(\xi_1^3 - \xi_2^3). \quad (62)$$

On the other hand, addition of Eqs. (61a) and (61b), and subsequent elimination of the trigonometric factor with that in Eq. (61c) by the identity  $\sin^2(\tilde{\phi}) + \cos^2(\tilde{\phi}) = 1$  gives

$$(x + y - 1)^2 + \bar{\gamma}^2(y - x)^2 = \left( \xi_2 \sqrt{\frac{y}{x}} + \xi_1 \sqrt{\frac{x}{y}} \right)^2. \quad (63)$$

Two-cluster fixed point solutions are given by the intersecting points of Eqs. (62) and (63). An example shown in Fig. 8 corresponding to the parameters  $\xi_1 = 0.9$  and  $\bar{\gamma} = 4.2$ . There are altogether four intersecting points, but two of them, namely  $(0, 0)$  and  $(1, 1)$ , do not correspond to the answers we seek ( $(0, 0)$  is the unstable incoherent state and  $(1, 1)$  is the one-cluster locked state solution). For the other two solutions, indicated as  $A$  and  $B$  in Fig. 8, we find that  $B$  corresponds to an unstable fixed point, while  $A$  is stable, and our numerical tests on Eqs. (61) and (43) show that  $A$  satisfies both types of stability, (i) and (ii) mentioned at the end of Sec. XB. Thus  $A$  is an attractor.

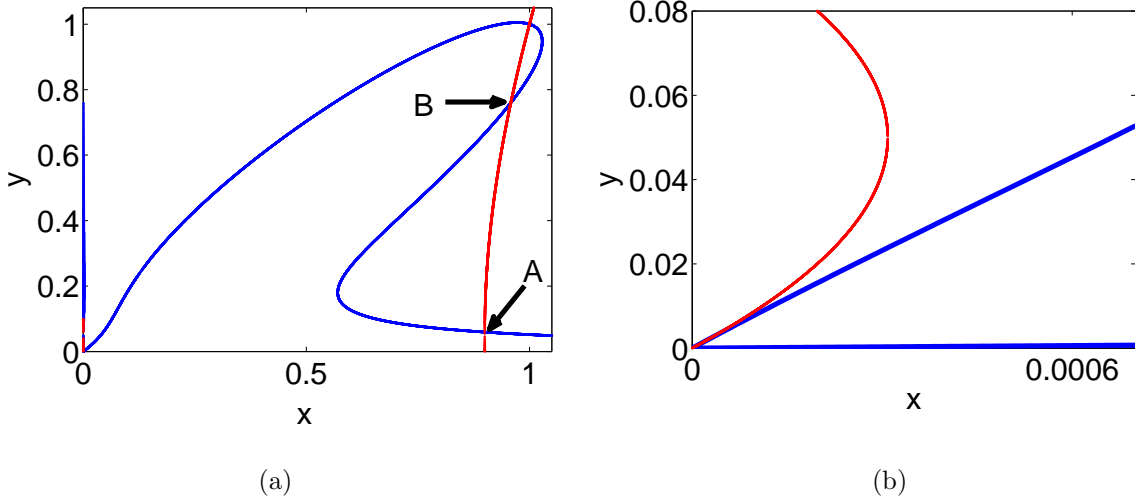


FIG. 8: (Color online) (a) Two-cluster locked state solutions. The blue line shows the curve for Eq. (63), and the red line shows the curve for Eq. (62); parameters:  $\xi_1 = 0.9$ ,  $\bar{\gamma} = 4.2$ . (b) Blowup of the figure in (a) around  $(0, 0)$ .

## 2. Two-cluster periodic solutions of Eq. (61)

In general, the two-cluster periodic solutions of Eq. (61) are hard to obtain analytically. However, in the case of large  $\bar{\gamma}$ , we can proceed using perturbation theory. If  $\bar{\gamma} \gg 1$  and  $\tilde{\rho}_1^2 - \tilde{\rho}_2^2$  is not small, then  $d\tilde{\phi}/d\hat{t}$  is very large, so  $\cos(\tilde{\phi})$  is rapidly varying. Thus, to lowest order in  $\bar{\gamma}^{-1}$ , we can neglect the  $\cos(\tilde{\phi})$  terms in the equations for  $d\tilde{\rho}_1/d\hat{t}$  and  $d\tilde{\rho}_2/d\hat{t}$ ,

$$\frac{d\tilde{\rho}_{1,2}^{(0)}}{d\hat{t}} = (\xi_{1,2} - \tilde{\rho}_{1,2}^{(0)^2})\tilde{\rho}_{1,2}^{(0)}, \quad (64)$$

and  $\tilde{\rho}_1^{(0)}$  and  $\tilde{\rho}_2^{(0)}$ , are attracted to  $\tilde{\rho}_1^{(0)} = \sqrt{\xi_1}$ ,  $\tilde{\rho}_2^{(0)} = \sqrt{\xi_2}$ , respectively. Thus we have

$$\frac{d\tilde{\phi}}{d\hat{t}} \approx -\bar{\gamma}(\xi_1 - \xi_2) - \frac{\xi_1^2 + \xi_2^2}{\sqrt{\xi_1\xi_2}} \sin(\tilde{\phi}), \quad (65)$$

which, for large  $\bar{\gamma}$  has the solution,

$$\tilde{\phi} \approx \tilde{\phi}_0 - \bar{\gamma}(\xi_1 - \xi_2)\hat{t} + \frac{\xi_1^2 + \xi_2^2}{\sqrt{\xi_1\xi_2}} \cos[\tilde{\phi}_0 - \bar{\gamma}(\xi_1 - \xi_2)\hat{t}]. \quad (66)$$

To next order in  $\bar{\gamma}^{-1}$ , we write  $\tilde{\rho}_{1,2} = \tilde{\rho}_{1,2}^{(0)} + \tilde{\rho}_{1,2}^{(1)}$  where the perturbation  $\tilde{\rho}_1^{(1)}$  to the lowest order quantity  $\tilde{\rho}_1^{(0)}$  satisfies

$$\frac{d\tilde{\rho}^{(1)}}{d\hat{t}} = -2\xi_1\tilde{\rho}_1^{(1)} + \xi_2^{3/2} \cos[\tilde{\phi}_0 - \bar{\gamma}(\xi_1 - \xi_2)\hat{t}]. \quad (67)$$

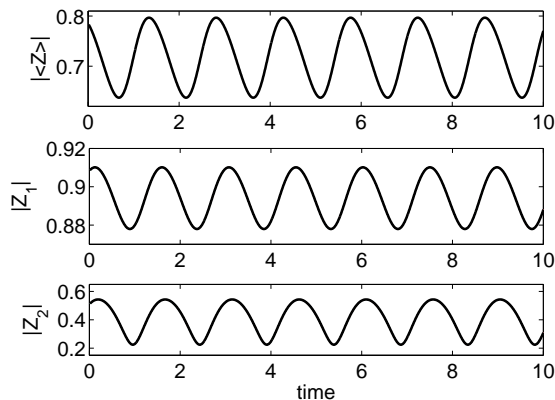


FIG. 9: Simulation study of a two-cluster periodic state; parameters:  $N = 50000$ ,  $\xi_1 = 0.8$ ,  $\bar{\gamma} = 7.2$ .

The homogeneous solution of the above equation decays as  $e^{-2\xi_1 t}$ , and thus does not contribute to the time periodic attractor. For large  $\bar{\gamma}$  the inhomogeneous term varies with a period  $2\pi/[\bar{\gamma}(\xi_1 - \xi_2)]$  which, since  $\bar{\gamma}$  is large, is much shorter than the damping time  $(2\xi_1)^{-1}$ . Thus for calculating the inhomogeneous solution, we may neglect the term  $2\xi_1\tilde{\rho}_1^{(1)}$ .

This yields

$$\tilde{\rho}_1^{(1)}(\hat{t}) = -\frac{\xi_2^{3/2}}{\bar{\gamma}(\xi_1 - \xi_2)} \sin[\tilde{\phi}_0 - \bar{\gamma}(\xi_1 - \xi_2)\hat{t}], \quad (68)$$

and similarly

$$\tilde{\rho}_2^{(1)}(\hat{t}) = -\frac{\xi_1^{3/2}}{\bar{\gamma}(\xi_1 - \xi_2)} \sin[\tilde{\phi}_0 - \bar{\gamma}(\xi_1 - \xi_2)\hat{t}]. \quad (69)$$

Thus  $\rho_{1,2}^{(1)}$  are indeed small compared to  $\rho_{1,2}^{(0)}$ , if  $\xi_1 \neq \xi_2$  and  $\bar{\gamma}$  is sufficiently large. Hence we obtain a two cluster time periodic state whose frequency is, to lowest order,  $\bar{\gamma}(\xi_1 - \xi_2)$ . Figure 9 shows long-time results of a simulation of Eq. (43) with 50000 oscillators, and with parameters  $\xi_1 = 0.8$  and  $\bar{\gamma} = 7.2$ , for a periodic attractor. Comparison of these results with the approximate analytical solution above shows good agreement.

In order to see why this solution represents an attractor of the full  $N$  dimensional system (43), we consider its Lyapunov exponents. To lowest order the individual clusters are uncoupled locked states. We have already shown (Sec. IX) that a single-cluster locked state of a system of  $N$  oscillators has  $N - 1$  negative exponents (having possible values  $-1, -2, -3$ ) and one zero exponent that corresponds to a rigid rotation in the complex plane of the entire

system of  $N$  oscillators (i.e.,  $\hat{z}_j \rightarrow \hat{z}_j \exp(i\Phi)$  for constant  $\Phi$ ). Thus, to lowest order in our  $\bar{\gamma}^{-1}$  expansion, there are  $(N_1 - 1) + (N_2 - 1) = N - 2$  negative Lyapunov exponents and two zero Lyapunov exponents. Now introducing small coupling between the clusters (i.e., finite  $\bar{\gamma}$ ), the negative exponents will be slightly perturbed by an amount  $\bar{\gamma}^{-1} \ll 1$  and hence will remain negative. The only danger of instability is that one of the two zero exponents might be perturbed to be a positive number of order  $\bar{\gamma}^{-1}$ . However, this cannot be the case, because the full system must have two zero exponents, and thus the two zero exponents of the lowest order uncoupled approximation are preserved. To see this, we note that there is one zero exponent corresponding to a rigid rotation of the entire system of  $N = N_1 + N_2$  oscillators. Note that this zero exponent is not present in the three ODE's, Eq. (61), for  $\tilde{\rho}_1, \tilde{\rho}_2$  and  $\tilde{\phi}$ , since a rigid rotation ( $\tilde{\theta}_1 \rightarrow \tilde{\theta}_1 + \Phi, \tilde{\theta}_2 \rightarrow \tilde{\theta}_2 + \Phi$ ) does not change  $\tilde{\phi} = \tilde{\theta}_1 - \tilde{\theta}_2$ . Another zero exponent results from the fact that the time periodic flow, Eq. (61), has a zero exponent corresponding to displacement along its orbit. Thus we conclude that our large- $\bar{\gamma}$ , two-cluster, states are attractors.

#### D. Cluster-states with $C \geq 3$

##### 1. Do locked state attractors with three or more clusters exist?

The above implies that, at large  $\Gamma$ , we can have both two-cluster and single-cluster locked state attractors. A natural question is whether large- $\Gamma$  locked state attractors with  $C > 2$  clusters are possible. We now give a partial answer to this question by ruling out the possibility of locked states composed of more than three clusters. To rule out  $C > 3$  locked state solutions of Eq. (43), we substitute the locked-state ansatz  $Z_c(\hat{t}) = \tilde{\rho}_c e^{i\tilde{\theta}_{c0}} e^{-i\Omega\hat{t}}$  into (43), where  $\tilde{\rho}_c > 0$  and  $\tilde{\theta}_{c0}$  are time independent real constants. This yields

$$\langle Z(\hat{t}) \rangle = \langle Z(0) \rangle e^{-i\Omega\hat{t}}, \quad \text{and} \quad (70a)$$

$$[(1 + i\bar{\gamma})\tilde{\rho}_c^2 - i\Omega]\tilde{\rho}_c e^{i\tilde{\theta}_{c0}} = \langle Z(0) \rangle \quad (70b)$$

Multiplying Eq. (70b) by its complex conjugate, we obtain

$$\tilde{\rho}_c^2 [\tilde{\rho}_c^4 + (\bar{\gamma}\tilde{\rho}_c^2 - \Omega)^2] = |\langle Z(0) \rangle|^2. \quad (71)$$

A particular state corresponds to particular values of  $\Omega$  and  $|\langle Z(0) \rangle|$ . Thus Eq. (71) must be satisfied for each individual cluster  $c$  composing the state for the same values of  $\Omega$  and  $|\langle Z(0) \rangle|$ . Since (71) is a cubic equation for  $\tilde{\rho}_c^2$ , there can be at most three real values of  $\tilde{\rho}_c > 0$ . Furthermore, Eq. (70) uniquely determines the value of  $\tilde{\theta}_{c0}$  for each value of  $\tilde{\rho}_c$ . We, therefore, conclude that large- $\Gamma$ , locked, cluster states with  $C > 3$  cannot occur. This leaves open the question of whether or not three cluster locked state attractors exist. In this regard, we note that in our, admittedly limited, series of numerical experiments we have so far not seen such attractors.

## 2. Periodic, quasiperiodic and chaotic attractors for $C \geq 3$

Considering the  $C$  complex ODE's for the  $C$  cluster states, Eq. (58), and again introducing a polar representation,  $Z_c = \tilde{\rho}_c \exp(i\tilde{\theta}_c)$ , we obtain a  $2C - 1$  dimensional dynamical system of  $C$  real equations for  $d\tilde{\rho}_c/d\hat{t}$  and  $C - 1$  real equations for  $d\tilde{\phi}_c/d\hat{t}$  where  $\tilde{\phi}_c = \tilde{\theta}_c - \tilde{\theta}_1$  and  $c = 2, \dots, C$ . Again taking  $\bar{\gamma} \gg 1$ , we find  $C - 1$  lowest order angle evolutions,

$$\frac{d\tilde{\phi}_c^{(0)}}{d\hat{t}} = \Delta\omega_c, \quad \Delta\omega_c = -\bar{\gamma}(\xi_c - \xi_1). \quad (72)$$

Assuming that the set of  $C - 1$  frequencies  $\{\Delta\omega_c\}$  are irrationally related in the sense that the equation,

$$\sum_{c=1}^{C-1} m_c \Delta\omega_c = 0, \quad (73)$$

has no solution where the  $m_c$  are positive or negative integers except for the trivial solution where  $m_c = 0$  for all  $c$ , then we can think of the lowest order solution as being  $(C - 1)$ -quasiperiodic in the  $2C - 1$  cluster-state phase space  $\{\rho_1, \dots, \rho_C; \phi_2, \dots, \phi_C\}$ . Application of perturbation theory in the small parameter  $\bar{\gamma}^{-1}$  is mathematically equivalent to the problem of investigating the introduction of small coupling between  $C - 1$  oscillators.

For example, for three clusters, we have the possibility of two-frequency quasiperiodic motion, and the possibly analogous problem of introducing small *generic* coupling between two periodic oscillators was originally addressed by Arnold [45] in his study of the circle map,  $\Xi_{n+1} = (2\pi R_0 + \Xi_n + \kappa \sin \Xi_n) \bmod 2\pi$ , where  $R_0$  denotes the rotation number for  $\kappa = 0$  ( $R_0$  is analogous to  $\Delta\omega_1/\Delta\omega_2$  in our case, and  $\kappa$  is analogous to  $\bar{\gamma}^{-1}$ ). Arnold's work resolved the problem of the convergence of perturbation theory of coupled oscillators which is plagued by

the proliferation of small denominators in higher and higher order terms in the perturbation series. Results, both analytical (as by Arnold [45]) and numerical, show that for  $\kappa < 1$ , attracting quasiperiodic motion continues to exist on a positive Lebesgue measure of the parameter space (in our case, the parameter-space is  $\{\xi_c; \bar{\gamma}\}$ ), but is structurally unstable: for any parameter set yielding two-frequency quasiperiodicity, one can find an arbitrarily close-by set of parameters where the motion is periodic. Alternatively, one can say that two-frequency quasiperiodic attractors exist on a positive Lebesgue measure Cantor set in parameter-space, while periodic attractors exist on the complement of this set which is an open set (e.g., see [21] for further discussion).

Figure 10 shows evidence supporting this scenario. The figure shows the result of numerical computations of (58) for the rotation number defined by

$$R_c = \lim_{T \rightarrow \infty} \frac{\theta_2(T) - \theta_1(T)}{\theta_3(T) - \theta_1(T)}, \quad (74)$$

versus the rotation number at infinite  $\bar{\gamma}$ ,

$$R_0 = \frac{\xi_2 - \xi_1}{\xi_3 - \xi_1}, \quad (75)$$

for  $C = 3, \bar{\gamma} = 30, \xi_3 = 0.2, \xi_1$  varied from 0.497 to 0.533, and  $\xi_2 = 1 - \xi_1 - \xi_3$ . A classic “devil’s staircase” pattern is clearly observed, with periodic orbits corresponding to frequency-locking plateaus at rational rotation numbers of  $R_c = 2/3, 5/7, 3/4$ , and  $4/5$ . The blowups, shown in Figs. 10(b) and 10(c), reveal further plateaus at  $R_c = 7/10$  and  $7/9$ , suggesting that (as in Arnold’s circle map) plateaus exist for all rational numbers  $p/q$  ( $p, q$  incommensurate integers) with the plateau widths decreasing as  $q$  increases.

The case  $C - 1 \geq 3$  adds a new ingredient. Again, as  $\bar{\gamma}^{-1}$  increases from zero ( $\bar{\gamma}$  becomes finite),  $(C - 1)$ -quasiperiodic attractors generally persist on a positive Lebesgue measure Cantor set in parameter space, but the open complement of this Cantor set now typically contains a variety of other types of attractors, including periodic attractors (as for  $C = 3$ ), chaotic attractors, and  $M$ -frequency quasiperiodic attractors with  $M < C - 1$  ([46]-[49]). In particular, the generic existence of structurally stable chaotic attractors resulting from perturbations to  $P$ -frequency quasiperiodic attractors for  $P \geq 3$  has been proven by Newhouse, Ruelle and Takens [46, 47].

Note that all the motions, including the chaotic motions, referred to above occur in the context of Eq. (58) and are therefore motions of the  $C$  clusters. Also note that in our

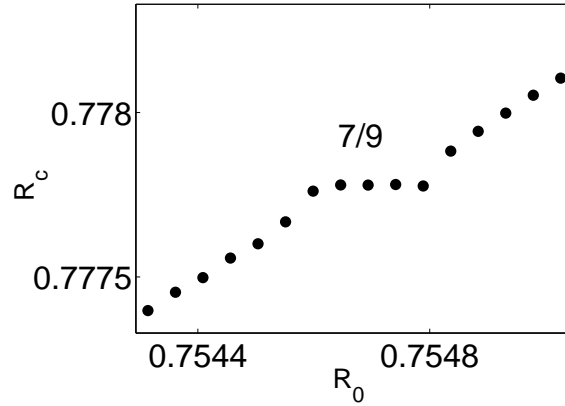
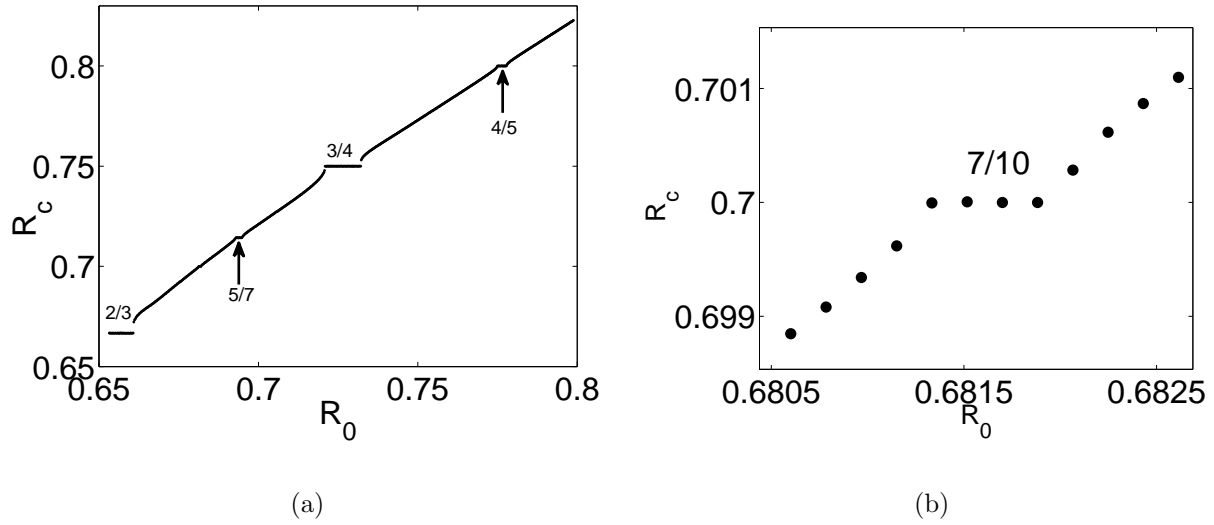


FIG. 10: (a) Rotation number  $R_c$  from numerical solutions versus the infinite  $\bar{\gamma}$  rotation number  $R_0$  for  $C = 3$ ,  $\bar{\gamma} = 30$ ,  $\xi_3 = 0.2$ , and  $\xi_1$  varied from 0.497 to 0.533 with  $\xi_2 = 1 - \xi_1 - \xi_3$ . (b), (c) Blowup of two regions of the figure in (a).

discussion above of solutions of Eq. (58), we have treated the parameters  $\{\xi_c\}$  as continuous. While this is formally allowed for Eq. (58), we emphasize that if we consider that (58) is derived from system (43) with finite  $N$ , then  $\xi_c = N_c/N$  can only take on discrete values (although they may be very dense for large  $N$ ).

## XI. DISCUSSION AND CONCLUSIONS

In this paper we have studied some properties of large all-to-all coupled Landau-Stuart oscillator networks. The motivation for studying this class of systems is to reveal possible generic behaviors of large systems of coupled oscillators where the oscillators have both amplitude and phase degrees of freedom.

In the first half of this paper (Secs. III-VII), motivated by experiments reported in Ref. [2], we studied stability of the incoherent state ( $\langle z \rangle = 0$ ) and determined the stability / instability boundary for different cases. First, we studied networks with spread in the distributions of the natural oscillator frequencies  $\omega$  and the linear amplitude growth parameter  $\alpha$ , but with no nonlinear frequency shift contribution, i.e.,  $\gamma_i = 0$  for all oscillators  $i$ . Second, we studied networks with no spread in the distribution  $\alpha$ , but with a constant nonlinear frequency shift parameter  $\bar{\gamma}$  for all oscillators. After establishing a mathematical framework to determine the stability / instability boundary, we characterized the changes in the stability / instability boundary that these modifications cause. First, we found that a spread  $\delta\alpha$  in the distribution of  $\alpha$  smooths out the discontinuity at  $\alpha = 0$  in the slope of the stability / instability boundary. Second, spread in  $\alpha$  causes the minimum of  $\Gamma_c$  to shift away from  $\bar{\alpha} = 0$  to  $\bar{\alpha} > 0$  when  $\delta\alpha > 0$ . Third, increase of the nonlinear frequency shift parameter  $\bar{\gamma}$  monotonically lowers  $\Gamma_c$ .

Similar to large networks of phase oscillators of the Kuramoto type, large networks of Landau-Stuart oscillators with small nonlinear frequency shifts have a tendency to always synchronize into a locked state exhibiting steady, constant-amplitude sinusoidal motion when the coupling strength is large enough. In order to better understand this behavior, in Secs. VIII-X we studied the limit  $\Gamma/\Gamma_c \rightarrow \infty$ . We found that as  $\Gamma/\Gamma_c \rightarrow \infty$ , Eq. (7) reduces to Eq. (43), which depends only on coupling among oscillators individually dominated by their constant nonlinear characteristics. Considering cluster state attractors of (43) we obtained the following results.

1. For sufficiently low values of the nonlinear frequency shift parameter ( $\bar{\gamma} < \sqrt{3}$ ), there is a unique, global attractor that is a single-cluster, locked state attractor.
2. For larger  $\bar{\gamma}$ , multiple-cluster attractors can occur, but the single-cluster, locked state attractor continues to exist.



3. For larger  $\bar{\gamma}$ , two-cluster locked state attractors exist, but locked state attractors with more than three clusters are never possible [50].
4. For  $C = 3$ , regions of parameter space exist where two frequency quasiperiodicity can occur with periodic attractors arbitrarily nearby in parameter space.
5. For  $C \geq 4$ ,  $(C - 1)$ -frequency quasiperiodicity can occur, and periodicity and chaos occur for parameter values near those yielding  $(C - 1)$ -frequency quasiperiodicity.

This work is supported by the U.S. Army Research Office grant # W911NF-12-1-0101.

**Appendix A: Theoretical values of the critical coupling strength with a uniformly distributed  $g(\omega)$**

In this appendix we summarize the theoretical results of the critical coupling strength  $\Gamma_c$  when  $g(\omega)$  is given by the uniform distribution

$$g(\omega) = \frac{1}{2}U(1 - |\omega|), \quad (\text{A1})$$

First, we determine  $\Gamma_c$  when there is no spread in  $h(\alpha)$ , i.e.,  $h(\alpha) = \delta(\alpha - \bar{\alpha})$ , and  $\gamma = 0$  for all oscillators. When  $\bar{\alpha} > 0$ , we have

$$\Gamma_c^{-1} = \frac{\pi}{4} + \frac{1}{2} \tan^{-1} \left( \frac{1}{2\bar{\alpha}} \right); \quad (\text{A2})$$

similarly, when  $\bar{\alpha} < 0$ , we have

$$\Gamma_c^{-1} = \tan^{-1} \left( \frac{1}{|\bar{\alpha}|} \right). \quad (\text{A3})$$

For the cases when there is spread in  $h(\alpha)$ , we assume the same model  $h(\alpha) = (2\delta\alpha)^{-1}U(\delta\alpha - |\alpha - \bar{\alpha}|)$ . By denoting  $\bar{\alpha}_+ = \bar{\alpha} + \delta\alpha$  and  $\bar{\alpha}_- = \bar{\alpha} - \delta\alpha$ , we have for  $\bar{\alpha} > \delta\alpha$ ,

$$\Gamma_c^{-1} = \frac{\pi}{4} + \frac{1}{4\delta\alpha} \left[ \bar{\alpha}_+ \tan^{-1} \left( \frac{1}{2\bar{\alpha}_+} \right) - \bar{\alpha}_- \tan^{-1} \left( \frac{1}{2\bar{\alpha}_-} \right) + \frac{1}{4} \ln \left| \frac{4\bar{\alpha}_+^2 + 1}{4\bar{\alpha}_-^2 + 1} \right| \right]; \quad (\text{A4})$$

for  $\bar{\alpha} < \delta\alpha$ ,

$$\Gamma_c^{-1} = -\frac{1}{2\delta\alpha} \left[ \bar{\alpha}_+ \tan^{-1} \left( \frac{1}{\bar{\alpha}_+} \right) - \bar{\alpha}_- \tan^{-1} \left( \frac{1}{\bar{\alpha}_-} \right) + \frac{1}{2} \ln \left| \frac{\bar{\alpha}_+^2 + 1}{\bar{\alpha}_-^2 + 1} \right| \right]; \quad (\text{A5})$$

and for  $|\bar{\alpha}| < -\delta\alpha$ ,

$$\Gamma_c^{-1} = I_1 + I_2, \quad \text{where} \quad (\text{A6a})$$

$$I_1 = \frac{\pi}{4} \left( \frac{\bar{\alpha}_+}{2\delta\alpha} \right) + \frac{1}{4\delta\alpha} \left[ \bar{\alpha}_+ \tan^{-1} \left( \frac{1}{2\bar{\alpha}_+} \right) + \frac{1}{4} \ln |4\bar{\alpha}_+^2 + 1| \right], \quad (\text{A6b})$$

$$I_2 = -\frac{1}{2\delta\alpha} \left[ -\bar{\alpha}_- \tan^{-1} \left( \frac{1}{\bar{\alpha}_-} \right) - \frac{1}{2} \ln |\bar{\alpha}_-^2 + 1| \right]. \quad (\text{A6c})$$

Similar to the results with a Lorentzian  $g(\omega)$ , it can be readily shown that Eqs. (A4)-(A5) reduce to Eqs. (A2) and (A3) in the limit  $\delta\alpha \rightarrow 0$ .

Next, we determine  $\Gamma_c$  when there is no spread in  $h(\alpha)$ , i.e.,  $h(\alpha) = \delta(\alpha - \bar{\alpha})$  where  $\bar{\alpha}$  is constant, and the nonlinear frequency parameter  $\bar{\gamma}$  is a nonzero constant for all oscillators. For  $\bar{\alpha} < 0$ , we know that  $\bar{\gamma}$  does not affect stability of the state  $\langle z \rangle = 0$ , so  $\Gamma_c$  is still given by Eq. (A3). For  $\bar{\alpha} > 0$ , we have, by substituting  $s = i\Omega$  into the final expression after integration in Eq. (25), and introducing  $\eta_{\pm} = \Omega \pm 1 + \bar{\alpha}\bar{\gamma}$ , that  $\Gamma_c$  and  $\Omega$  are to be given by the solution of the following pair of equations,

$$-4\Gamma_c^{-1} = \frac{\bar{\gamma}}{2} \ln \left| \frac{\eta_+^2(\eta_-^2 + 4\bar{\alpha}^2)}{\eta_-^2(\eta_+^2 + 4\bar{\alpha}^2)} \right| - \left[ \pi + \tan^{-1} \left( \frac{\eta_+}{2\bar{\alpha}} \right) - \tan^{-1} \left( \frac{\eta_-}{2\bar{\alpha}} \right) \right], \quad (\text{A7a})$$

$$0 = \bar{\gamma} \left[ \pi - \tan^{-1} \left( \frac{\eta_+}{2\bar{\alpha}} \right) + \tan^{-1} \left( \frac{\eta_-}{2\bar{\alpha}} \right) \right] + \frac{1}{2} \ln \left| \frac{\eta_+^2(\eta_+^2 + 4\bar{\alpha}^2)}{\eta_-^2(\eta_-^2 + 4\bar{\alpha}^2)} \right|. \quad (\text{A7b})$$

It can be easily checked from (A7) that  $\Gamma_c$  reduces to (A2) when  $\bar{\gamma} \rightarrow 0$  (Note  $\Omega \rightarrow 0$  in this limit).

- 
- [1] A. Pikovsky, M. Rosenblum and J. Kurths, *Synchronization: A Universal Concept in Non-linear Sciences*, Chapter 7 (Cambridge University Press, 2004).
  - [2] A. F. Taylor, M. R. Tinsley, F. Wang, Z. Huang and K. Showalter, *Sci.*, **323**, 614 (2009).
  - [3] S. Strogatz, *Sync: The Emerging Science of Spontaneous Order* (Hyperion 2003).
  - [4] G. Kozyreff, A. G. Vladimirov and P. Mandel, *Phys. Rev. Lett.* **85**, 3809 (2000).
  - [5] K. Wiesenfeld, C. Brawcikowski, G. James and R. Roy, *Phys. Rev. Lett.* **65**, 1749 (1990).
  - [6] J. Zamora-Munt, C. Masoller, J. Garcia-Ojalvo and R. Roy, *Phys. Rev. Lett.* **105**, 264101 (2010).

- [7] S. A. Marvel and S. H. Strogatz, *Chaos* **19**, 013132 (2009).
- [8] S. Nichols and K. Wiesenfeld, *Phys. Rev. A* **45**, 8430 (1992).
- [9] S. Dano, F. Hynne, S. DeMonte, F. d'Ovidio, P. G. Sorensen and H. Westerhoff, *Faraday Discussions* **120**, 261 (2002).
- [10] S. De Monte, F. d'Ovidio, S. Dano and P. G. Sorensen, *Proc. Natl. Acad. Sci. U.S.A.* **104**, 18377 (2007).
- [11] D. C. Michaels, E. P. Matyas and J. Jalife, *Circulation Research* **61**, 704 (1987).
- [12] S.H. Strogatz, D.M. Abrams, A.McRobie, B. Eckhardt and E.Ott, *Nature* **438**, 43 (2005).
- [13] B. Eckhardt, E. Ott, S. H. Strogatz, D. M. Abrams and A. McRobie, *Phys. Rev. E* **75**, 021110 (2007).
- [14] M. Abdulrehem and E. Ott, *Chaos* **19**, 013129 (2009).
- [15] I. Z.Kiss, Y. Zhai and J. L. Hudson, *Sci.* **296**, 1676 (2002).
- [16] S. Yamaguchi, H. Isejima, T. Matsuo, R. Okura, K. Yagita, M. Kobayashi and H. Okamura, *Sci.* **302**, 1408 (2003).
- [17] Y. Kuramoto, *International Symposium on Mathematical Problems in Theoretical Physics*, Lecture Notes in Physics, vol.39, edited by H. Araki (Springer-Verlag, Berlin, 1975).
- [18] Y. Kuramoto, *Chemical Oscillations, Waves, and Turbulence* (Springer, Berlin, 1984).
- [19] J. A. Acebron, L. L. Bonilla, C. J. P. Vincente, F. Ritort and R. Spigler, *Rev. Mod. Phys.* **77**, 137 (2005).
- [20] S. H. Strogatz, *Physica D* **143**, 1 (2000).
- [21] E. Ott, *Chaos in Dynamical Systems*, 2nd edition, Chapter 6, section 6.5 (Cambridge University Press, New York, 2002).
- [22] E. Ott and T. M. Antonsen, *Chaos* **18**, 037113 (2008); *Chaos* **19**, 023117 (2009).
- [23] M. Shiino and M. Frankowicz, *Phys. Lett. A* **136**, 103 (1989).
- [24] G. B. Ermentrout, *Physica D* **41**, 219 (1990).
- [25] R. E. Mirollo and S. H. Strogatz, *J. Stat. Phys.* **60**, 245 (1990).
- [26] P. C. Matthews and S. H. Strogatz, *Phys. Rev. Lett.* **65**, 1701 (1990).
- [27] P. C. Matthews, R. E. Mirollo and S. H. Strogatz, *Physica D* **52**, 293 (1991).
- [28] H. Daido and K. Nakanishi, *Phy. Rev. Lett.* **93**, 104101 (2004).
- [29] D. Pazó and E. Montbrió, *Phys. Rev. E*, **73**, 055202 (2006).
- [30] In general, however, we note that  $\omega$  and  $\alpha$  can be expected to have correlations; e.g., even if

the physical parameter vector  $\mathbf{p}$  has dimension  $n \geq 2$  and the variation of components of  $\mathbf{p}$  are uncorrelated, we can still expect that the particular functional dependences, Eq. (3), of the oscillator parameters on the physical parameters will induce correlations between  $\omega$  and  $\alpha$ .

- [31] In addition to the situation of many coupled Landau-Stuart equations, oscillator death occurs very generally for many types of coupled oscillator situations, including coupling between only a few oscillators (e.g., two). As an example of one of the many references on this topic, we note the recent paper, Ref. [32], and references therein.
- [32] J. J. Suárez-Vargas, J. A. González, A. Stefanovska and P. V. McClintock, *Europhys. Lett.* **85**, 38008 (2009).
- [33] O. E. Omel'chenko and M. Wolfrum, *Phys. Rev. Lett.* **109** 164101 (2012).
- [34] Equation (29) [together with a transformation of the form of the interaction term to that of Eq. (8)] can also be used to generalize previous work of Ref. [28] on the “aging transition” to include dispersion of the natural frequencies.
- [35] It can be shown that when  $h(\alpha) = \delta(\alpha - 1)$ ,  $\Gamma_c^{-1} = \pi g(0)$  for any general unimodal frequency distribution  $g(\omega)$  symmetric about  $\omega = 0$  (see Ref. [27]).
- [36] E. Montbrió and D. Pazó, *Phys. Rev. Lett.* **106**, 254101 (2011).
- [37] V. Hakim and W.-J. Rappel, *Phys. Rev. A*, **46**, R7347 (1992).
- [38] N. Nakagawa and Y. Kuramoto, *Prog. Theor. Phys.* **89** 313 (1993).
- [39] N. Nakagawa and Y. Kuramoto, *Physica D* **75**, 74 (1994).
- [40] N. Nakagawa and Y. Kuramoto, *Physica D* **80**, 307 (1995).
- [41] H. Daido and K. Nakanishi, *Phys. Rev. Lett.* **96**, 054101 (2006).
- [42] K. Kaneko *Physica D* **41**, 137 (1990).
- [43] K. Kaneko *Physica D* **54**, 5 (1991).
- [44] L. Yu, E. Ott and Q. Chen, *Physica D* **53**, 102 (1991); *Phys. Rev. Lett.* **65**, 2935 (1990).
- [45] V. I. Arnold, *AMS Transl. Series 2*, **46** 213 (1965).
- [46] S. Newhouse, D. Ruelle, and F. Takens, *Comm. Math. Phys.* **64**, 35 (1978).
- [47] D. Ruelle and F. Takens, *Comm. Math. Phys.* **20**, 167 (1971).
- [48] C. Grebogi, E. Ott and J. A. Yorke, *Phys. Rev. Lett.* **51**, 339 (1983).
- [49] C. Grebogi, E. Ott and J. A. Yorke, *Physica D* **15**, 354 (1985).
- [50] We do not yet know whether  $C = 3$  locked state attractors exist, but we have so far not

observed them in our simulations.